A Perylene Five-membered Ring Diimide for Organic Semiconductors and π-Expanded Conjugated Molecules

Liangliang Chen [a,b], Botao Wu[c], Liyuan Qin [a,b], Yan-Ying Huang [a,b], Wei Meng [a,b], Ruirui Kong[d], Xiaobo Yu [a,b], Kaiyuan ChenChai [a,b], Cheng Li [a], Guanxin Zhang [a], Xi-Sha Zhang[a,b,*], Deqing Zhang [a,b,*]

[a] Beijing National Laboratory for Molecular Sciences, CAS Key Laboratory of Organic Solids, CAS Center of Excellence in Molecular Science, Institute of Chemistry, Chinese Academy of Sciences, Beijing 100190, P. R. China;

[b] University of Chinese Academy of Sciences, Beijing 100049, P. R. China;

[c] College of Chemistry and Molecular Engineering, Peking University, Beijing, 100871, P. R. China;

[d] State Key Laboratory of Metastable Materials Science and Technology, Yanshan University, Qinhuangdao, 066004, P. R. China.

CONTENTS

1. Materials

The reagents and starting materials were commercially available and used as received otherwise specified elsewhere. The commercially available "compound" **4** (Scheme 1 and Scheme S1) from Zhengzhou Alfa Company is the mixture of perylene-3,9-dicarboxylic acid and perylene-3,10-dicarboxylic acid and their molar ratio was about 1:1 based on the ^{1}H NMR analysis. Hexyl isocyanate was purchased from Shanghai Aladdin Bio-Chem Technology Co., LTD. Compound **6** (Scheme 2) was synthesized according to literature. [S1]

2. Characterization techniques

Column chromatography was used to purify the materials and the 200-300 mesh silica gel was purchased from Chemical Industry Research Institute of Yantai and used as received. Thin layer chromatography used to monitor the reactions and preparative thin layer chromatography to separate the compounds were also purchased from Chemical Industry Research Institute of Yantai.

^{1}H NMR and ^{13}C NMR spectra were measured with Bruker AVANCE III 400 MHz, AVANCE III 500 MHz, Bruker AVANCE NEO 600 MHz and Bruker AVANCE NEO 700 MHz spectrometers. High resolution mass spectral (HRMS) data were collected on either 9.4T Solarix Mass instrument or APEX II Mass instrument. Elemental analyses (EA) were performed on a Carlo-Erba-1106 instrument.

Absorption spectra of solutions were recorded on HITACHI UH4150 spectrophotometer. Emission spectra of solutions were recorded on Hitachi FP-6000 spectrometer. Fluorescence quantum yield of solution and solid were measured on HAAMATSU C11347. Cyclic voltammetry measurements were carried out on CHI660C instrument at room temperature in a three-electrode cell by using glassy carbon as the working electrode, Pt wire as auxiliary electrode, and Ag/AgCl (saturated KCl) as reference electrode; the scan rate was 100 mV s^{-1}, and n-Bu_4NPF_6 (0.1 mol/L in anhydrous dichloromethane) was used as the supporting electrolyte. For calibration, the redox potential of ferrocene/ferrocenium (Fc/Fc^{+}) was measured under the same conditions as internal or external standard. HOMO and LUMO energies of these molecules were estimated with the following equations: HOMO = -(E_{ox}^{onset} + 4.8) eV, LUMO = -(E_{red}^{onset} + 4.8) eV.

Single crystals used for X-ray diffraction analysis were obtained by slowly diffusing methanol into the chloroform solution or toluene solution. The data for the single crystals of **PDI39**, **PDI39-CN** and **2** were collected with a Rigaku Saturn diffractometer with CCD area detector with Cu at 170 K. Crystallographic data reported in this paper were deposited in the Cambridge Crystallographic Data Centre (CCDC No. 2003562 for compound **PDI39**; CCDC No. 2094430 for compound **PDI39-CN** and CCDC No.2074735 for compound **2**).

3. Synthesis and characterizations

3.1 Synthesis of PDI39

Scheme S1. Synthetic route of compound **PDI39**

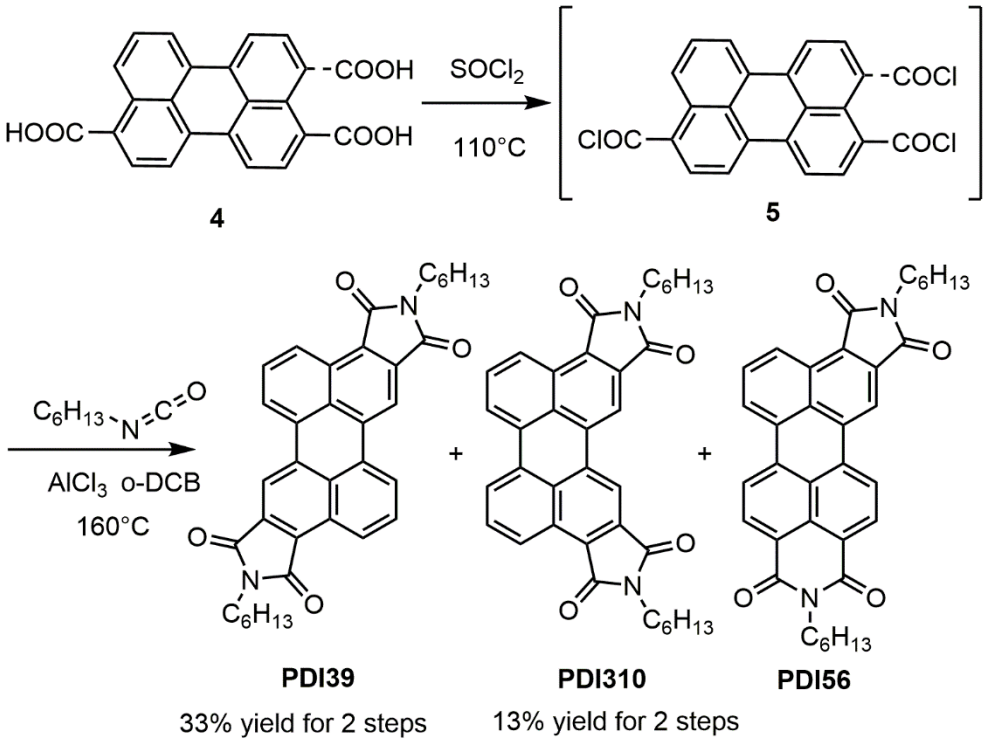

*Characterization of "compound" **4***

^{1}H NMR (600 MHz, DMSO-d_6, 298 k) δ ppm: 13.24 (s, 2H), 8.89 (d, J = 8.6 Hz, 1H), 8.81 (d, J = 8.6 Hz, 1H), 8.54 (d, J = 7.6 Hz, 1H), 8.50 (q, J = 8.3, 7.9 Hz, 3H), 8.17 (dd, J = 7.9, 4.0 Hz, 2H), 7.71 (q, J = 8.5 Hz, 2H). HRMS (ESI) m/z: $[M-H]^-$ calcd for $C_{22}H_{11}O_4$ 339.0663, Found 339.0663.

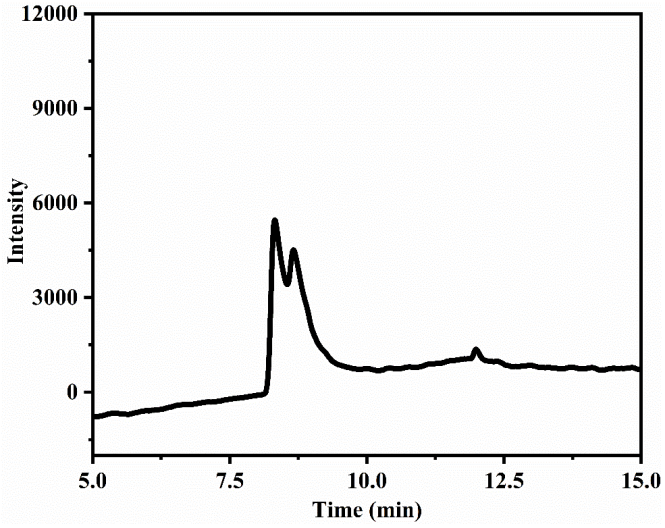

Figure S1-1. HPLC chromatograms of "compound" **4** in MeOH solution.

*Synthesis of **PDI39**, **PDI310** and **PDI56***

To a 250 mL round-bottom flask equipped with a magnetic stir bar and a cooling condenser, the mixture of perylene-3,9-dicarboxylic acid and perylene-3,10-dicarboxylic acid (the molar ratio of perylene-3,9-dicarboxylic acid and erylene-3,10-dicarboxylic acid was about 1:1 according to the ^{1}H NMR data) (**4**, 1 g, 2.9 mmol) and thionyl chloride (20 mL) were added. The mixture was heated at 110 ^{o}C (oil bath) for 12 h. After cooling to room temperature, the excess thionyl chloride was removed under reduced pressure. The residue was transferred into Schlenk tube (100 mL) and then aluminum chloride (2.4 g, 17.6 mmol) and 1,2-dichlorobenzene (30 mL) were added. The mixture was stirred at room temperature for 3 min. and then hexyl isocyanate (5.6 g, 44.1 mmol) was added. After that, the reaction tube was sealed and the mixture was heated at 160 ^{o}C (oil bath) for 24 h. After cooling to room temperature, the solvent was removed by rotary evaporation. The residue was purified by column chromatography with petroleum ether (b.p. 60-90 ^{o}C) and dichloromethane (1:1, v/v) as eluent to give a crude product. The crude product was recrystallized three times by chloroform and methanol to give compound **PDI39** as an orange solid (534 mg, 33% yield), PDI310 as a red solid (210 mg, 13% yield). The residue was purified by column chromatography with dichloromethane as eluent to give compound PDI56 as a dark-red solid.

PDI39: ^{1}H NMR (500 MHz, $C_2D_2Cl_4$, 353.2 K) δ (ppm): 8.97 (d, *J*=8.0 Hz, 2H), 8.57 (s, 2H), 8.51 (d, *J*=7.0 Hz, 2H), 7.83 (t, *J*=8.0 Hz, 2H), 3.79 (t, *J*=7.5 Hz, 4H), 1.84-1.78 (m, 4H), 1.48-1.37(m, 12H), 0.96 (t, *J*=7.0 Hz, 6H); ^{13}C NMR (125 MHz, $C_2D_2Cl_4$, 353.2 K) δ (ppm): 168.9, 168.3, 137.0, 132.6, 131.0, 130.8, 129.9, 129.5, 126.7, 126.1, 124.8, 113.8, 38.3, 31.4, 28.6, 26.6, 22.5, 13.9; HRMS (MALDI-TOF) m/z: $[M]^+$ calcd for $C_{36}H_{34}N_2O_4$ 558.2513, Found 558.2522; Elemental Anal. Calcd for $C_{36}H_{34}N_2O_4$: C, 77.40; H, 6.13; N, 5.01; Found: C, 77.26; H, 6.13; N, 5.08.

PDI310: ^{1}H NMR (500 MHz, $CDCl_3$, 298 K) δ (ppm): 8.69 (d, *J* = 8.2 Hz, 2H), 8.29 (d, *J* = 7.6 Hz, 2H), 8.23 (s, 2H), 7.68 (t, *J* = 7.9 Hz, 2H), 3.74 (t, *J* = 7.5 Hz, 4H), 1.76 (p, *J* = 7.5 Hz, 4H), 1.43-1.33 (m, 12H), 0.92 (t, *J* = 7.0 Hz, 6H); ^{13}C NMR (100 MHz, $CDCl_3$, 298 K) δ (ppm): 168.1, 167.5, 134.8, 131.1, 130.1, 129.7, 129.6, 128.3, 125.8, 124.5, 122.9, 113.5, 38.2, 31.5, 28.7, 26.7, 22.6, 14.1; HRMS (MALDI-TOF) m/z: $[M]^+$ calcd for $C_{36}H_{34}N_2O_4$ 558.2513, Found 558.2521; Elemental Anal: Calcd for $C_{36}H_{34}N_2O_4$: C, 77.40; H, 6.13; N, 5.01. Found: C, 77.20; H, 6.20; N, 5.00.

PDI56: ^{1}H NMR (400 MHz, $CDCl_3$, 298 K) δ (ppm): 8.73 (d, *J* = 8.4 Hz, 1H), 8.33 (d, *J* = 8.0 Hz, 2H), 8.21-8.17 (m, 2H), 8.10 (t, *J* = 9.3 Hz, 2H), 7.63 (t, *J* = 7.9 Hz, 1H), 4.14 (t, *J* = 7.7 Hz, 2H), 3.73 (t, *J* = 7.4 Hz, 2H), 1.79-1.72 (m, 4H), 1.52-1.33 (m, 12H), 0.94-0.87 (m, 6H); ^{13}C NMR (176 MHz, $CDCl_3$, 298 K) δ 168.7, 168.0, 163.3, 163.3, 135.4, 135.3, 134.9, 131.9, 131.3, 131.1, 130.5, 129.8, 129.8, 129.1, 127.1, 127.0, 126.0, 125.1, 122.8, 122.3, 121.8, 121.2, 115.0, 40.6, 38.3, 31.6, 31.4, 28.7, 28.0, 26.9, 26.6, 22.6, 22.6, 14.1, 14.1. HRMS (MALDI-TOF) m/z: $[M+H]^+$ calcd for $C_{36}H_{35}N_2O_4$ 559.2591, Found 559.2592; Elemental Anal: Calcd for $C_{36}H_{34}N_2O_4$: C, 77.40; H, 6.13; N, 5.01. Found: C, 77.19; H, 6.19; N, 4.93.

Scheme S1-1. Synthetic route of compound **PDI310**

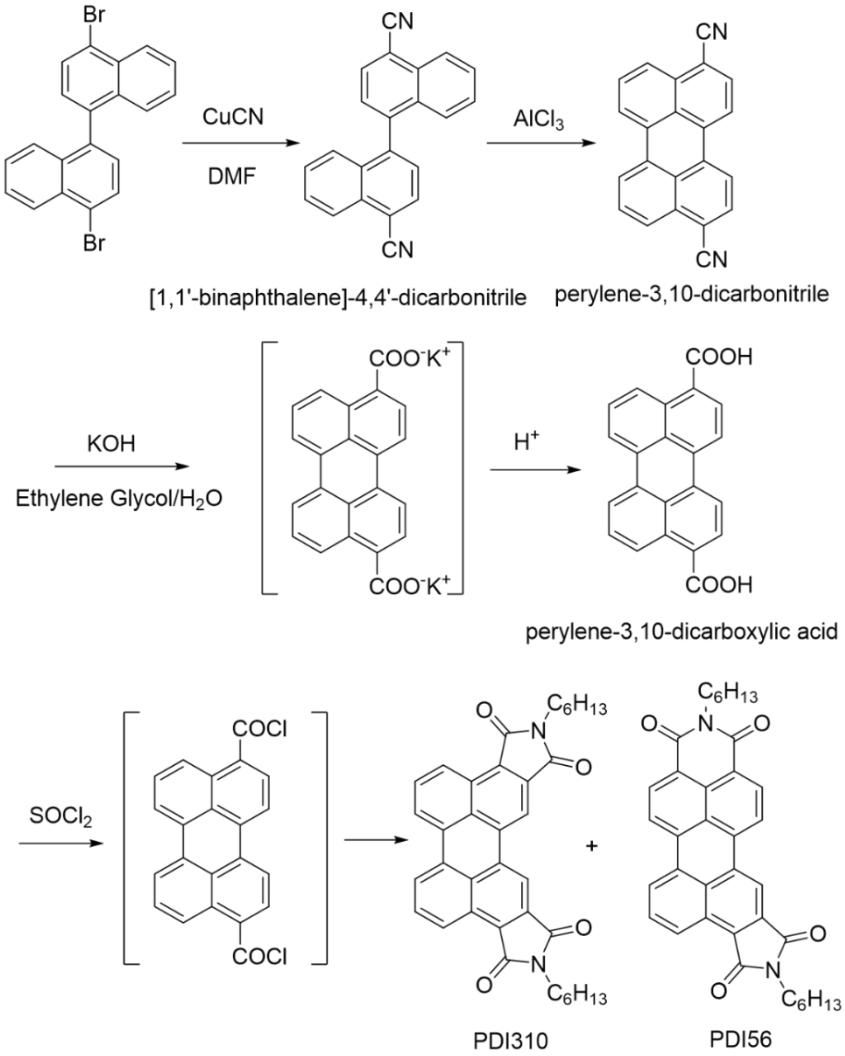

Synthesis of **[1,1'-binaphthalene]-4,4'-dicarbonitrile**

To a 250 mL round-bottom flask equipped with a magnetic stir bar, **4,4'-dibromo-1,1'-binaphthalene** (5 g, 12.1 mmol), CuCN (4 g, 45 mmol) and DMF (100 mL) were added. The mixture was degassed and charged with nitrogen for three times and then heated to 150 ^{o}C (oil bath) for 12 h. After cooling to room temperature, the reaction was quenched with ammonia solution (30 mL, 25%-28%) and MeOH (100 mL) and H_2O (30 mL) were added. A large amount of precipitation was emerged and fileted off directly. The crude product was then purified by flash column chromatography using petroleum ether (b.p. 60-90 ^{o}C) and dichloromethane (1:1, v/v) as eluent to give a white solid **[1,1'-binaphthalene]-4,4'-dicarbonitrile** (2.971 g, 81% yield).

^{1}H NMR (400 MHz, $CDCl_3$, 298K) δ 8.39 (d, *J* = 8.4 Hz, 2H), 8.06 (d, *J* = 7.3 Hz, 2H), 7.73 (td, *J* = 7.6, 1.2 Hz, 2H), 7.53 (d, *J* = 7.3 Hz, 2H), 7.47 (td, *J* = 7.8, 1.2 Hz, 2H), 7.37 (d, *J* = 8.5 Hz, 2H). HRMS (EI) m/z: calcd for $C_{22}H_{12}N_2$ 304.1000, Found 304.1003.

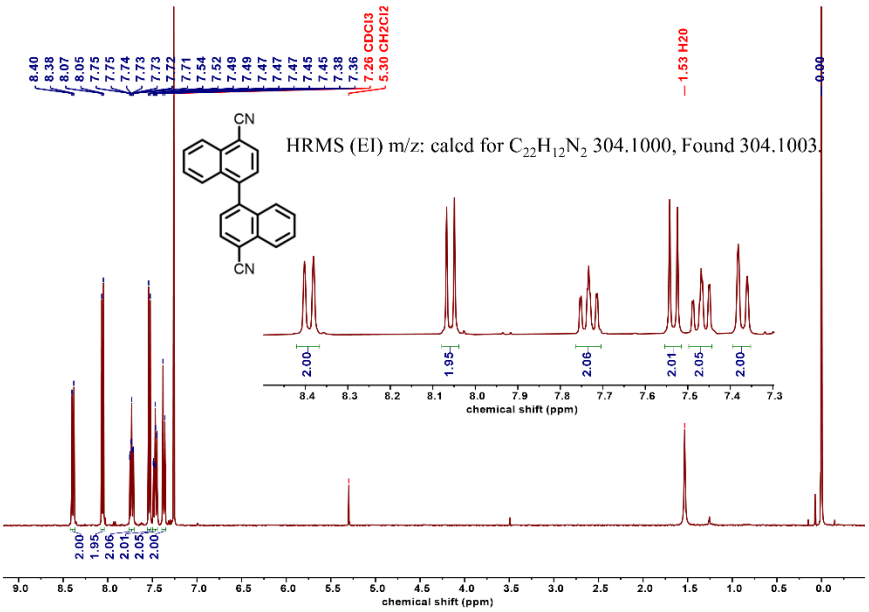

Figure S1-2. ^{1}H NMR spectrum of **[1,1'-binaphthalene]-4,4'-dicarbonitrile** (400 MHz, $CDCl_3$, 298 K)

Synthesis of **perylene-3,10-dicarbonitrile**

To a 100 mL round-bottom flask, **[1,1'-binaphthalene]-4,4'-dicarbonitrile** (2.5 g, 8.2 mmol) and $AlCl_3$ (15 g, 112 mmol) were added. The mixture was heated to 140 ^{o}C for 3 h under air atmosphere. After cooling to room temperature, 10% HCl solution (50 mL) were added slowly under ice bath. A large amount of precipitate was generated and filtered off. The precipitate was washed with water and methanol for several times. The solid was further purified by Soxhlet extraction using methanol to remove the impurities. The crude was used directly for next step.
HRMS (MALDI-TOF) m/z: $[M]^+$ calcd for $C_{22}H_{10}N_2$ 302.0844, Found 302.0846.

Synthesis of **perylene-3,10-dicarboxylic acid**

To a 100 mL round-bottom flask, **perylene-3,10-dicarbonitrile** (6.4 g, 21 mmol), KOH (30 g, 53 mmol), ethylene glycol (150 mL) and H_2O (20 mL) were added. The mixture was heated to 150 ^{o}C for 10 h under air atmosphere. After cooling to room temperature, the mixture was filtered off. The filtrate was neutralized by10% HCl solution and a large amount of precipitate was generated and filtered off. The precipitate was washed with water for several times. After drying under vacuum, the crude (4.5 g, 62% yield) was used directly for next step.
^{1}H NMR (400 MHz, DMSO-d_6, 298 K) δ ppm: 13.21 (s, 2H, br), 8.80 (d, J = 8.5 Hz, 2H), 8.50 (dd, J = 7.9, 5.1 Hz, 4H), 8.16 (d, J = 7.9 Hz, 2H), 7.70 (t, J = 8.1 Hz, 2H).
HRMS (ESI) m/z: $[M-H]^-$ calcd for $C_{22}H_{11}O_4$ 339.0663, Found 339.0662.

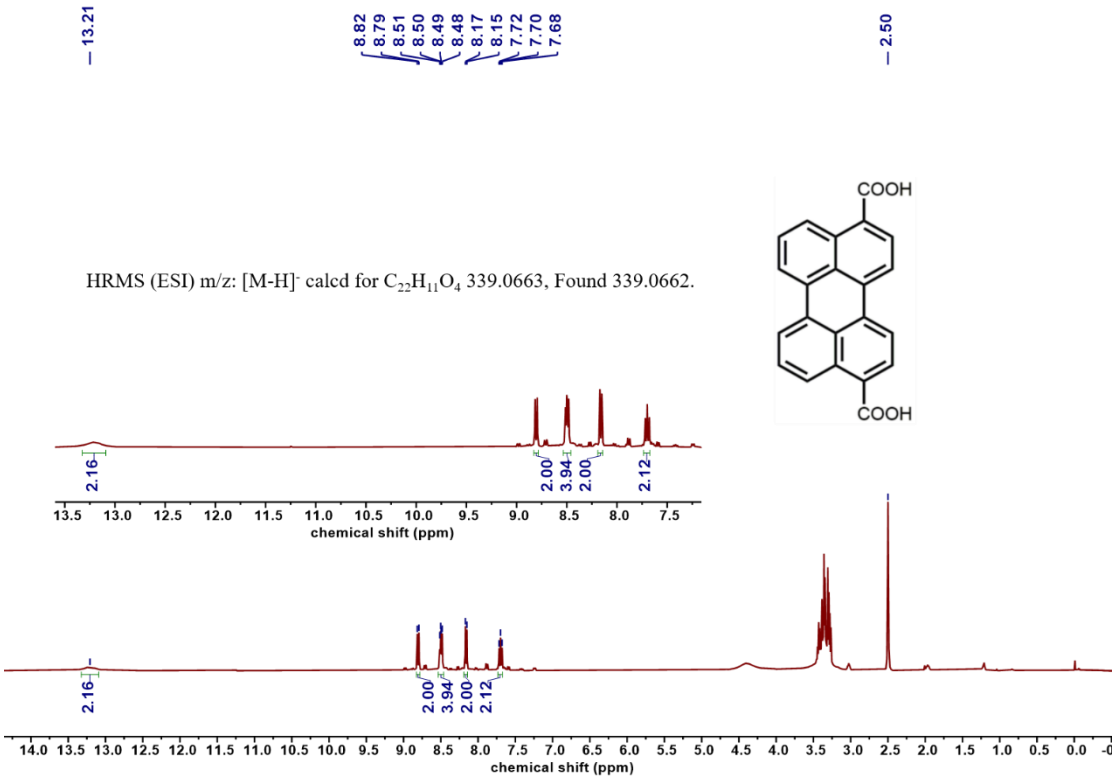

Figure S1-3. ^{1}H NMR spectrum of **perylene-3,10-dicarboxylic acid** (400 MHz, *d*$_6$-DMSO, 298 K).

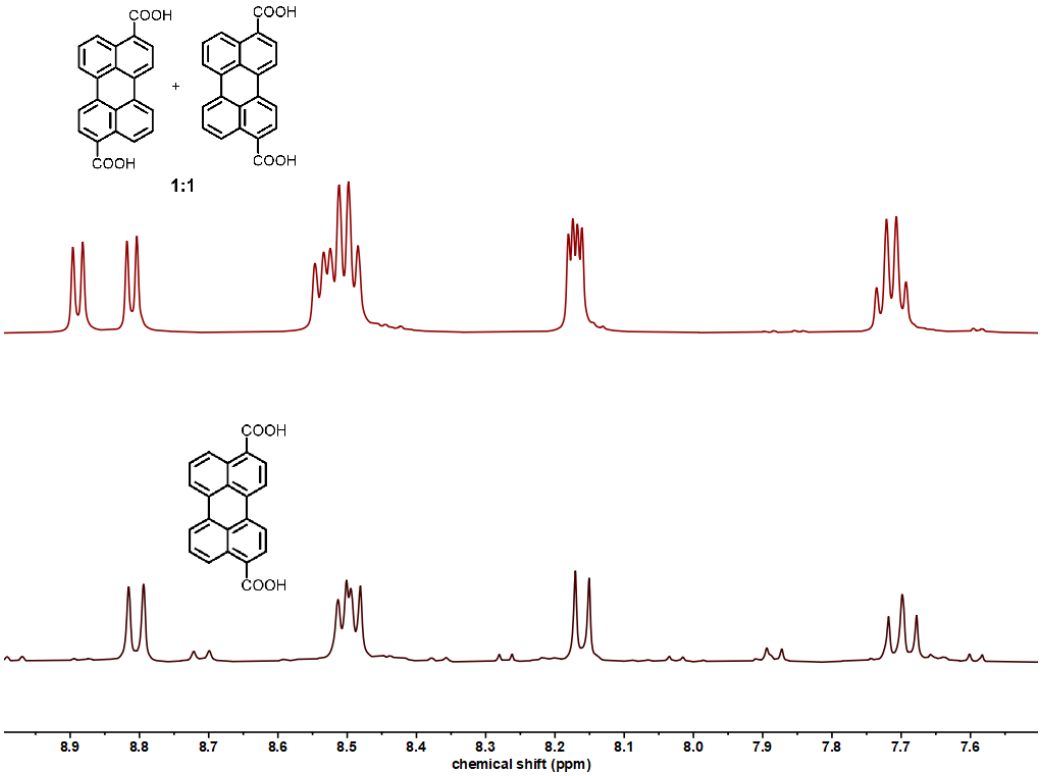

Figure S1-4. Enlarged ^{1}H NMR spectrum of "compound" **4** and compound **perylene-3,10-dicarboxylic acid**.

Synthesis of **PDI310 and PDI56**

To a 100 mL round-bottom flask equipped with a magnetic stir bar and a cooling condenser, the crude product of **perylene-3,10-dicarboxylic acid** (800 mg, 2.35 mmol) and thionyl chloride (15 mL) were added. The mixture was heated at 110 ºC (oil bath) for 12 h. After cooling to room temperature, the excess thionyl chloride was removed under reduced pressure. The residue was transferred into Schlenk tube (100 mL) and then aluminum chloride (1.877 g, 14 mmol) and 1,2-dichlorobenzene (20 mL) were added. The mixture was stirred at room temperature for 3 min. and then hexyl isocyanate (3.976 g, 47 mmol) was added. After that, the reaction tube was sealed and the mixture was heated at 160 ºC (oil bath) for 24 h. After cooling to room temperature, the solvent was removed by rotary evaporation. The residue was purified by column chromatography with petroleum ether (b.p. 60-90 ºC) and dichloromethane (1:1-0:1, v/v) as eluent to give a crude product. The crude product was recrystallized three times by chloroform and methanol to give compound **PDI310** as a red solid (330 mg, 25% yield), **PDI56** as a dark-red solid (378 mg, 29% yield).

Scheme S1-2. Synthetic route of compound **PDI39-CN**

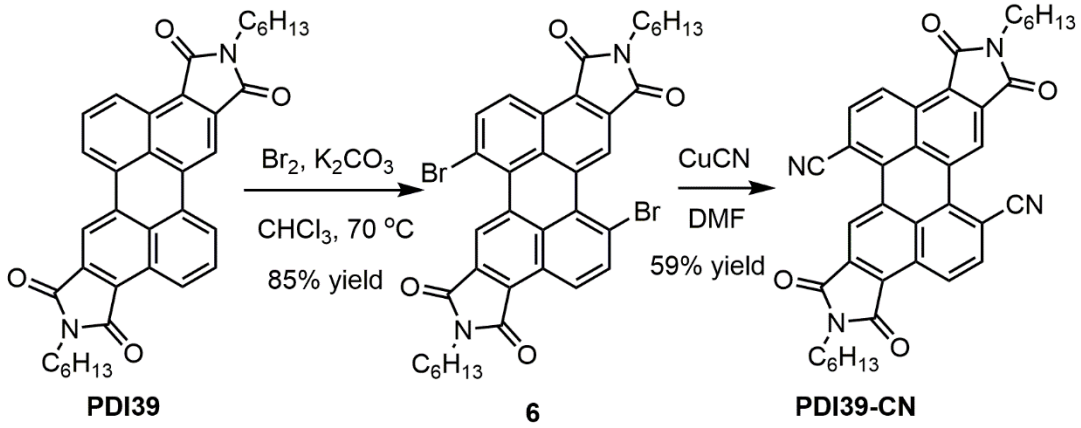

Synthesis of ***PDI39-Br***

To a 250 mL round-bottom flask equipped with a magnetic stir bar, **PDI39** (1 g, 1.8 mmol), potassium carbonate (1.5 g, 10.8 mmol) and chloroform (120 mL) were added. After bromine (5 mL, 97.4 mmol) was added quickly, the mixture was heated at 70 ºC (oil bath) for 6 days. After cooling to room temperature, the mixture was poured into saturated solution of sodium bisulfite, and the mixture was extracted with dichloromethane (50 mL×3) and washed with saturated solution of sodium bisulfite (50 mL×3). The organic layer was dried by anhydrous Na_2SO_4 and concentrated under reduced pressure. The crude product was then purified by flash column chromatography using petroleum ether (b.p. 60-90 ºC) and dichloromethane (1:1, v/v) as eluent to give **PDI39-Br** as an orange solid (1.1 g, 85% yield).

^{1}H NMR (400 MHz, $CDCl_3$, 298 K) δ (ppm): 9.16 (s, 2H), 8.69 (d, *J* = 8.8 Hz, 2H), 7.95 (d, *J* = 8.8 Hz, 2H), 3.76 (t, *J* = 7.2 Hz, 4H), 1.80-1.73 (m, 4H), 1.44-1.32 (m, 12H), 0.91 (t, *J* = 7.2 Hz, 6H); ^{13}C NMR (100 MHz, $CDCl_3$, 298 K) δ (ppm): 168.5, 167.9, 136.8, 134.2, 133.5, 130.7, 129.3, 126.9, 126.2, 125.8, 123.1, 120.1, 38.4, 31.4,

28.7, 26.6, 22.5, 14.0. HRMS (MALDI-TOF) m/z: $[M]^+$ calcd for $C_{36}H_{32}Br_2N_2O_4$ 714.0723, Found 714.0728.

Synthesis of ***PDI39-CN***

To a 50 mL round-bottom flask equipped with a magnetic stir bar, **PDI39-Br** (200 mg, 0.28 mmol), CuCN (126 mg, 1.4 mmol) and DMF (20 mL) were added. The mixture was degassed and charged with nitrogen for three times and then heated to 150 °C (oil bath) for 15 h. After cooling to room temperature, the reaction was quenched with ammonia solution (10 mL, 25%-28%), and the mixture was extracted with dichloromethane (30 mL× 3). The organic layer was dried by anhydrous Na_2SO_4 and concentrated under reduced pressure. The crude product was then purified by flash column chromatography using petroleum ether (b.p. 60-90 °C) and dichloromethane (1:1-1:5, v/v) as eluent to give an orange-red solid **PDI39-CN** (100 mg, 59% yield).

^{1}H NMR (400 MHz, $CDCl_3$, 298 K) δ (ppm): 9.48 (s, 2H), 9.19 (d, *J* = 8.6 Hz, 2H), 8.12 (d, *J* = 8.6 Hz, 2H), 3.80 (t, *J* = 7.4 Hz, 4H), 1.80-1.73 (m, 4H), 1.43-1.31 (m, 12H), 0.90 (d, *J* = 6.8 Hz, 6H); ^{13}C NMR (100 MHz, $CDCl_3$, 298 K) δ (ppm): 168.0, 166.8, 134.1, 133.9, 133.8, 130.9, 129.6, 127.9, 127.1, 120.4, 119.6, 109.9, 38.7, 31.4, 28.6, 26.6, 22.5, 14.0. HRMS (MALDI-TOF) m/z: $[M]^-$ calcd for $C_{38}H_{32}N_4O_2$ 608.2429, Found 608.2428; Elemental Anal. Calcd for $C_{38}H_{32}N_4O_4$: C, 74.98; H, 5.30; N, 9.20; Found: C, 75.00; H,5.32; N, 8.99.

3.2 Synthesis of 1 and 2

Scheme S2. Synthetic route of compound **1** and **2**

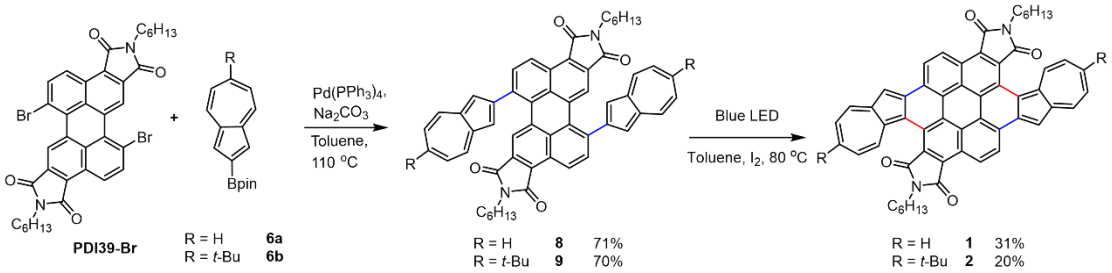

Synthesis of ***8***

To a 50 mL round-bottom flask equipped with a magnetic stir bar and a cooling condenser, **PDI39-Br** (200 mg, 0.28 mmol), **6a** (182 mg, 0.7 mmol), sodium carbonate (222 mg, 2.1 mmol) and Pd $(PPh_3)_4$ (16 mg, 0.01 mmol) were added. The mixture was degassed and charged with nitrogen for three times. Then toluene (15 mL), ethanol (5 mL) and water (5 mL) were added into the flask. The mixture was heated at 110 °C (oil bath) for 12 h. After cooling to room temperature, the reaction was quenched with water (10 mL), and the mixture was extracted with dichloromethane (30 mL× 3). The organic layer was dried by anhydrous Na_2SO_4 and concentrated under reduced pressure. The crude product was then purified by flash column chromatography using petroleum ether (b.p. 60-90 °C) and dichloromethane (2:1, v/v) as eluent to give a purple solid **8** (161 mg, 71% yield).

^{1}H NMR (400 MHz, $CDCl_3$, 298 K) δ (ppm): 8.75 (d, *J* = 8.6 Hz, 2H), 8.24 (d, *J* = 9.6 Hz, 4H), 7.78 (d, *J* = 8.6 Hz, 2H), 7.71 (s, 2H), 7.57 (t, *J* = 9.6 Hz, 2H), 7.39 (s, 4H),

7.18 (t, J = 9.6 Hz, 4H), 3.60 (t, J = 7.2 Hz, 4H), 1.67-1.62 (m, 4H), 1.32-1.27 (m, 12H), 0.86 (t, J = 6.8 Hz, 6H); ^{13}C NMR (100 MHz, $CDCl_3$, 298 K) δ (ppm):168.8, 167.8, 151.1, 141.9, 138.2, 137.6, 137.1, 136.5, 134.7, 133.5, 130.3, 129.2, 127.6, 125.1, 124.6, 124.1, 122.0, 116.5, 38.0, 31.4, 28.7, 26.6, 22.5, 14.0. HRMS (MALDI-TOF) m/z: $[M]^+$ calcd for $C_{56}H_{46}N_2O_4$ 810.3458, Found 810.3450.

*Synthesis of **9***

To a 50 mL round-bottom flask equipped with a magnetic stir bar and a cooling condenser, **PDI39-Br** (200 mg, 0.28 mmol), **6b** (217 mg, 0.7 mmol), sodium carbonate (222 mg, 2.1 mmol) and Pd $(PPh_3)_4$ (16 mg, 0.01 mmol) were added. The mixture was degassed and charged with nitrogen for three times. Then toluene (15 mL), ethanol (5 mL) and water (5 mL) were added into the flask. The mixture was heated at 110 °C (oil bath) for 12 h. After cooling to room temperature, the reaction was quenched with water (10 mL), and the mixture was extracted with dichloromethane (30 mL× 3). The organic layer was dried by anhydrous Na_2SO_4 and concentrated under reduced pressure. The crude product was then purified by flash column chromatography using petroleum ether (b.p. 60-90 °C) and dichloromethane (2:1, v/v) as eluent to give a purple solid **9** (182 mg, 70% yield).

^{1}H NMR (400 MHz, $CDCl_3$, 298 K) δ (ppm): 8.84 (d, J = 8.6 Hz, 2H), 8.16 (d, J = 10.4 Hz, 4H), 7.98 (s, 2H), 7.90 (d, J = 8.6 Hz, 2H), 7.35 (s, 4H), 7.33 (d, J = 10.4 Hz, 4H), 3.58 (t, J = 7.2 Hz, 4H), 1.62-1.58 (m, 4H), 1.47 (s, 18H), 1.31-1.24 (m, 12H), 0.85 (t, J = 6.0 Hz, 6H); ^{13}C NMR (100 MHz, $CDCl_3$, 298 K) δ (ppm): 168.6, 167.6, 161.1, 149.6, 140.1, 138.1, 136.6, 135.7, 134.5, 133.4, 129.7, 128.9, 127.3, 124.6, 124.2, 121.9, 121.5, 115.6, 38.2, 37.5, 31.4, 30.9, 28.1, 26.1, 22.0, 13.5. HRMS (MALDI-TOF) m/z: $[M]^+$ calcd for $C_{64}H_{62}N_2O_4$ 922.4710, Found 922.4714.

*Synthesis of **1***

To standard photocyclization glasswares (Wattecs) equipped with a magnetic stir bar was added **8** (15 mg, 0.02 mmol), iodine (20 mg, 0.075 mmol) and toluene (10 mL). The above reaction was repeated 2 times at the same time in two separated glasswares and combined for purification and separation (totally, **8** was 15 mg × 2, 0.04 mmol). The mixture was illuminated by blue LED lamp (40 W) for 72 h at 85 °C (heating module). The mixture was concentrated under reduced pressure. The crude product was then purified by flash column chromatography using dichloromethane as eluent to give a brown solid **1** (10 mg) in 31% yield.

^{1}H NMR (500 MHz, $C_2D_2Cl_4$, 373.2 K) δ (ppm): 9.81 (d, J = 8.5 Hz, 2H), 9.05 (d, J = 8.5 Hz, 2H), 8.73 (d, J = 8.0 Hz, 2H), 8.63 (d, J = 8.0 Hz, 2H), 8.15 (s, 2H), 7.74 (t, J = 9.5 Hz, 2H), 7.46 (t, J = 9.3 Hz, 2H), 7.33 (t, J = 8.8 Hz, 2H), 3.87 (t, J = 7.5 Hz, 4H), 1.90-1.85 (m, 4H), 1.56-1.51 (m, 4H), 1.42-1.32 (m, 8H), 0.90 (t, J = 6.5 Hz, 6H). ^{13}C NMR (176 MHz, $C_2D_2Cl_4$, 373.2 K) δ (ppm): 169.4, 168.9, 140.4, 140.1, 139.7, 137.8, 137.5, 137.0, 125.8, 125.1, 125.0, 124.8, 124.5, 124.2, 123.6, 122.8, 122.0, 120.0, 119.9, 116.7, 112.1, 38.3, 31.7, 29.1, 26.8, 22.6, 14.1. HRMS (MALDI-TOF) m/z: $[M]^-$ calcd for $C_{56}H_{42}N_2O_4$ 806.3145, Found 806.3154.

*Synthesis of **2***

To standard photocyclization glasswares (Wattecs) equipped with a magnetic stir

bar was added **9** (58 mg, 0.06 mmol), iodine (75 mg, 0.29 mmol) and toluene (15 mL). The above reaction was repeated 4 times at the same time in four separated glasswares and combined for purification and separation (totally, **9** was 58 mg × 4, 0.25 mmol). The mixture was illuminated by blue LED lamp (40 W) for 72 h at 85 °C (heating module). The mixture was concentrated under reduced pressure. The crude product was then purified by flash column chromatography using dichloromethane as eluent to give a brown solid **2** (45 mg, 20% yield).

^{1}H NMR (500 MHz, $C_2D_2Cl_4$, 373.2 K) δ (ppm): 9.74 (d, *J* = 8.5 Hz, 2H), 8.96 (d, *J* = 8.5 Hz, 2H), 8.74 (d, *J* = 10.0 Hz, 2H), 8.66 (d, *J* = 11.0 Hz, 2H), 8.08 (s, 2H), 7.77 (d, *J* = 11.0 Hz, 2H), 7.58 (d, *J* = 10.0 Hz, 2H), 3.96 (t, *J* = 7.0 Hz, 4H), 2.02-1.97 (m, 4H), 1.66 (s, 18H), 1.58-1.46 (m, 12H), 1.01 (t, *J* = 7.0 Hz, 6H); ^{13}C NMR (125 MHz, $C_2D_2Cl_4$, 373.2 K) δ (ppm): 168.3, 167.8, 159.7, 139.4, 138.1, 137.8, 135.7, 134.9, 124.6, 124.6, 124.3, 123.5, 123.2, 123.0, 122.5, 122.2, 121.0, 120.4, 119.3, 119.2, 116.1, 110.3, 37.3, 36.9, 30.4, 30.3, 27.5, 25.3, 21.1, 12.6. HRMS (MALDI-TOF) m/z: $[M]^+$ calcd for $C_{64}H_{58}N_2O_4$ 918.4397, Found 918.4396.

3.3 Synthesis of 3

Scheme S3. Synthetic route of compound **3**

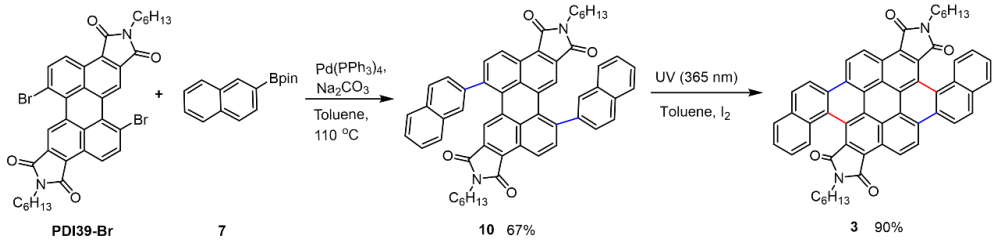

*Synthesis of **10***

To a 50 mL round-bottom flask equipped with a magnetic stir bar were added **PDI39-Br** (150 mg, 0.2 mmol), 4,4,5,5-tetramethyl-2-(2-naphthyl)-1,3,2-dioxaborolane (**7**, 170 mg, 0.67 mmol), sodium carbonate (175 mg, 1.7 mmol) and Pd $(PPh_3)_4$ (25 mg, 0.02 mmol). The mixture was degassed and charged with nitrogen for three times. Then toluene (15 mL), ethanol (5 mL) and water (5 mL) were added into the flask. The mixture was heated at 110 °C (oil bath) for 12 h. After cooling to room temperature, the reaction was quenched with water (10 mL), and the mixture was extracted with dichloromethane (30 mL×3). The organic layer was dried by anhydrous Na_2SO_4 and concentrated under reduced pressure. The crude product was then purified by flash column chromatography using petroleum ether (b.p. 60-90 °C) and dichloromethane (5:1-2:1, v/v) as eluent to give a red solid **10** (115 mg, 67% yield).

HRMS (MALDI-TOF) m/z: $[M]^-$ calcd for $C_{56}H_{46}N_2O_4$ 810.3463, Found 810.3460.

*Synthesis of **3***

To standard photocyclization glasswares (Wattecs) equipped with a magnetic stir bar was added **10** (20 mg, 0.025mmol), iodine (20 mg, 0.075 mmol) and toluene (15 mL). The above reaction was repeated 4 times at the same time in four separated glasswares and combined for purification and separation (totally, **10** was 20 mg × 4, 0.1mmol). The mixture was illuminated by UV light (365 nm, 250 W) for 30 min at room temperature and large amount of precipitation was emerged. The mixture was

filtered directly and washed with toluene, chloroform for several times. The product was dried to give an orange-red solid **3** (72 mg, 90% yield)

^{1}H NMR (700 MHz, $C_2D_2Cl_4$, 373.2 K) δ (ppm): 10.27 (d, *J* = 8.4 Hz, 2H), 9.86 (d, *J* = 9.0 Hz, 2H), 9.33 (d, *J* = 9.0 Hz, 2H), 8.74 (d, *J* = 8.4 Hz, 2H), 8.51 (d, *J* = 9.0 Hz, 2H), 8.25 (d, *J* = 8.4 Hz, 2H), 7.76 (t, *J* = 7.3 Hz, 2H), 7.63 (t, *J* = 7.3 Hz, 2H), 3.88-3.85 (m, 2H), 3.80-3.76 (m, 2H), 1.89-1.84 (m, 4H), 1.56-1.52 (m, 4H), 1.43-1.40 (m, 8H), 0.95 (t, *J* = 7.0 Hz, 6H); HRMS (MALDI-TOF) m/z: $[M]^-$ calcd for $C_{56}H_{42}N_2O_4$ 806.3150, Found 806.3150.

4. Photophysical and electrochemical properties of PDI39 and PDI39-CN

The UV, FL and CV of PDI39 and PDI39-CN

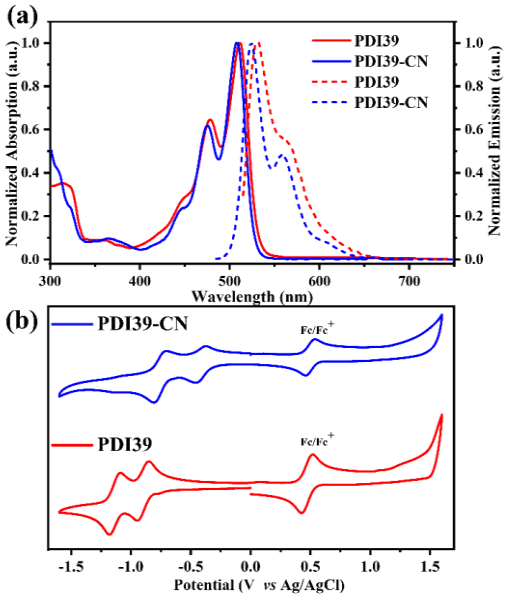

Figure S1. (a) Absorption (solid line) and emission spectra (dashed line) of **PDI39** and **PDI39-CN** in chloroform solution (10^{-5} mol/L); (b) Cyclic voltammograms of anhydrous dichloromethane solution of **PDI39** and **PDI39-CN** with ferrocene as internal standard at a scan rate of 100 mVs^{-1}. Glassy carbon electrode was used as working electrode, Pt as counter electrode and Ag/AgCl (saturated KCl) as reference electrode; n-Bu_4NPF_6 (0.1 M) in CH_2Cl_2 as supporting electrolyte.

Table S1. Summary of photophysical and electrochemical data of **PDI39** and **PDI39-CN**

Compound	E_{red1}^{onset} (V) [a]	λ_{max}(nm) [b]	λ_{onset}(nm) [b]	$\lambda_{max}^{emission}$ (nm) [c]	Eg^{opt}(eV) [d]	LUMO (eV) [e]	HOMO (eV) [e]	$\Phi_{F,sov}$ [f]	$\Phi_{F,solid}$ [g]
PDI39	**-0.81**	**510**	**534**	**530**	**2.32**	**-3.52**	**-5.84**	**45.90%**	**5.20%**
PDI39-CN	**-0.3**	**508**	**533**	**524**	**2.33**	**-4.03**	**-6.36**	**99.50%**	**4.00%**

[a] Cyclic voltammograms of anhydrous dichloromethane solution of **PDI39** and **PDI39-CN** at a scan rate of 100 mVs^{-1}. Glassy carbon was used as working electrode and Pt was used as counter electrode and Ag/AgCl (saturated KCl) as reference electrode; n-Bu_4NPF_6 (0.1 M) in anhydrous dichloromethane solution as supporting electrolyte; [b] Absorption wavelength in $CHCl_3$ (10^{-5} mol/L); [c] Emission wavelength in $CHCl_3$ (10^{-5} mol/L); [d] $E_g^{opt} = 1240/\lambda_{onset}$; (e) LUMO energy levels were calculated from $E_{LUMO} = -(4.80 + E_{red1}^{onset})$ eV, HOMO energy levels were calculated from $E_{HOMO} = (E_{LUMO}-E_g^{opt})$ eV; (f) Absolute fluorescence quantum yield in $CHCl_3$ (10^{-5} mol/L); (g) Absolute fluorescence quantum yield of solid.

5. Calculations on electronic properties

5.1 Electronic transitions of 2 and 3

For the geometry optimization and electronic property study, all calculations were conducted by using Gaussian 09 program[S2]. The geometry optimization and frequency analysis were performed by B3LYP/6-311G** or B3LYP(D3BJ)[S3]/def2-TZVP[S4] level of theory. Time-dependent density functional theory (TDDFT) calculation was performed at (TD)B3LYP/6-311G**[S5]level to obtain electronic excited states and simulation the UV-Vis spectrum. Natural transition orbits theory (NTO)[S6] was then used for the qualitative description of electronic transitions.

S2. Frisch, M. J.; Trucks, G. W.; Schlegel, H. B.; Scuseria, G. E.; Robb, M. A.; Cheeseman, J. R.; Scalmani, G.; Barone, V.; Mennucci, B.; Petersson, G. A.; Nakatsuji, H.; Caricato, M.; Li, X.; Hratchian, H. P.; Izmaylov, A. F.; Bloino, J.; Zheng, G.; Sonnenberg, J. L.; Hada, M.; Ehara, M.; Toyota, K.; Fukuda, R.; Hasegawa, J.; Ishida, M.; Nakajima, T.; Honda, Y.; Kitao, O.; Nakai, H.; Vreven, T.; Mont-gomery, J. A., Jr.; Peralta, J. E.; Ogliaro, F.; Bearpark, M.; Heyd, J. J.; Brothers, E.; Kudin, K. N.; Staroverov, V. N.; Kobayashi, R.; Nor-mand, J.; Raghavachari, K.; Rendell, A.; Burant, J. C.; Iyengar, S. S.; Tomasi, J.; Cossi, M.; Rega, N.; Millam, N. J.; Klene, M.; Knox, J. E.; Cross, J. B.; Bakken, V.; Adamo, C.; Jaramillo, J.; Gomperts, R.; Stratmann, R. E.; Yazyev, O.; Austin, A. J.; Cammi, R.; Pomelli, C.; Ochterski, J. W.; Martin, R. L.; Morokuma, K.; Zakrzewski, V. G.; Voth, G. A.; Salvador, P.; Dannenberg, J. J.; Dapprich, S.; Daniels, A. D.; Farkas, Ö.; Foresman, J. B.; Ortiz, J. V.; Cioslowski, J.; Fox, D. J. *Gaussian 09*, Revision E.01; Gaussian, Inc.: Wallingford, CT, 2013.

S3. (a) Lee, C.; Yang, W.; Parr, R. G., *Matter Mater. Phys.* 1988, ***37***, 785. (b) Miehlich, B.; Savin, A.; Stoll, H.; Preuss, H., *Chem. Phys. Lett.* 1989, ***157***, 200. (c) Becke, A. D., *J. Chem. Phys.* 1993, ***98***, 5648. (d) Grimme, S.; Ehrlich, S.; Goerigk, L., *J. Comput. Chem.* 2011, ***32***, 1456. (e) Grimme, S.; Antony, J.; Ehrlich, S.; Krieg, H., *J. Chem. Phys.* 2010, ***132***, 154104.

S4. Weigend, F.; Ahlrichs, R. *Phys., Chem. Chem. Phys.* 2005, ***7***, 3297-3305.

S5. (a) Hehre, W. J.; Ditchfield, R.; Pople, J. A., *J. Chem. Phys*. 1972, ***56***, 2257. (b) Hariharan, P. C.; Pople, J. A., *Theor. Chim. Acta.* 1973, ***28***, 213.

S6. Martin, R. L., *J. Chem. Phys*. 2003, ***118***, 4775.

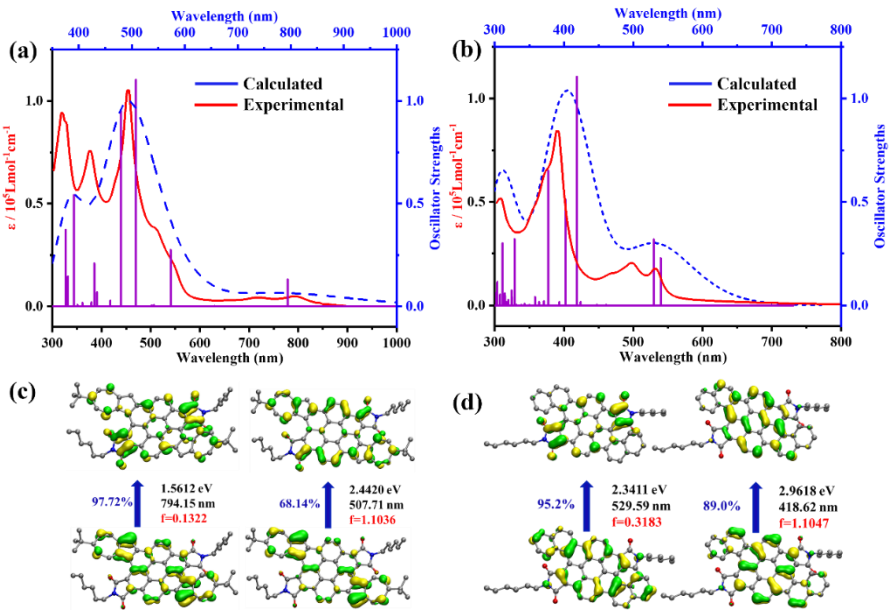

Figure S2. (a, b) absorption spectra of **2** (a) and **3** (b) in $CHCl_3$ (10^{-5} mol/L, red solid line), the simulated absorptions oscillator strengths (purple solid line) and simulated absorptions spectra (blue dash line); (c, d) Natural transition orbitals (NTO) of **2** (c) and **3** (d) based on DFT calculations.

Table S2. TDDFT results for compound **2**

state	λ (nm)	f	filled MO	empty MO	%
S_1	794.15	0.1322	HOMO	LUMO	97.2
S_2	573.15	0.2752	HOMO-2	LUMO	85.1
			HOMO	LUMO+3	11.7
S_3	507.71	1.1036	HOMO	LUMO+3	50.8
			HOMO-1	LUMO+2	21.8
			HOMO	LUMO+4	14.3
			HOMO-2	LUMO	9.4
S_4	479.50	0.9535	HOMO	LUMO+4	38.2
			HOMO	LUMO+3	29.9
			HOMO-1	LUMO+2	17.7
			HOMO-1	LUMO+1	7.2

Table S3. TDFT results for compound **3**

state	λ (nm)	f	filled MO	empty MO	%
S_1	539.53	0.2278	HOMO	LUMO	92.3
S_2	529.59	0.3183	HOMO-1	LUMO	92.6
S_3	418.62	1.1047	HOMO	LUMO+2	87.6

5.2 Aromaticity of 2

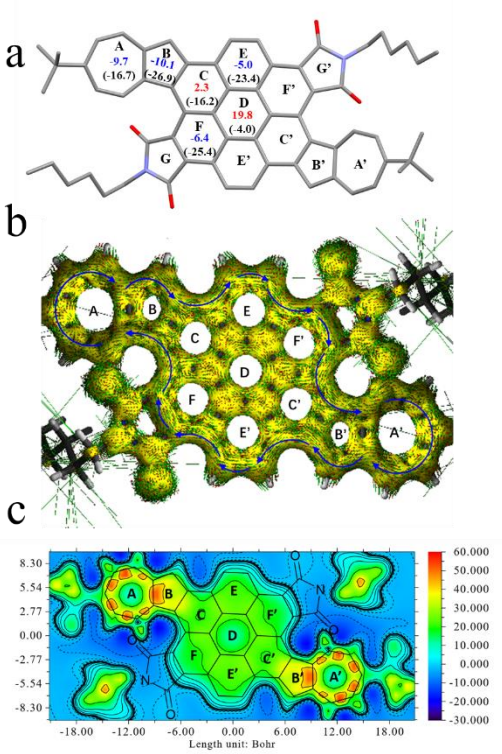

Figure S3. (a) Nucleus Independent Chemical Shift (NICS) value of **2** obtained by DFT calculations; (b) Calculated ACID plots for **2**. The diamagnetic (clockwise) ring currents are highlighted by blue under the magnetic field parallel to the z-axis; (C) Isotropic Chemical Shielding Surface at 1 Å of Z axis (ICSS(1)zz) for **2**; the deep orange region shows strong aromaticity.

5.3 Frontier orbitals and HOMO/LUMO energy levels of PDI39, PDI-CN, PDI and 1-3

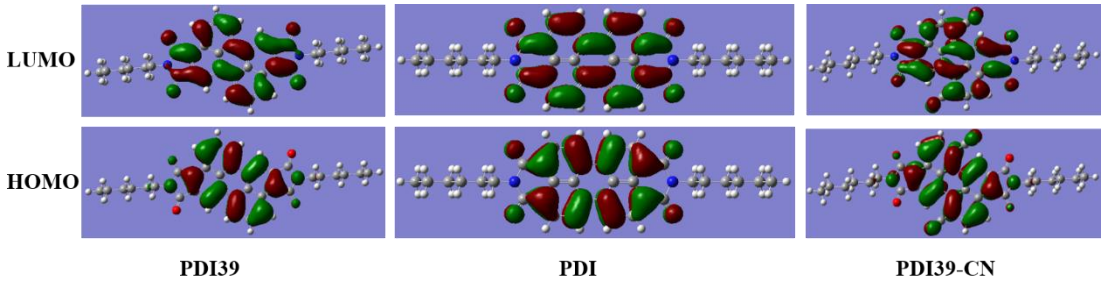

Figure S4. Frontier orbitals of **PDI39**, **PDI** and **PDI39-CN** based on DFT calculation at b3lyp/6-31g** level.

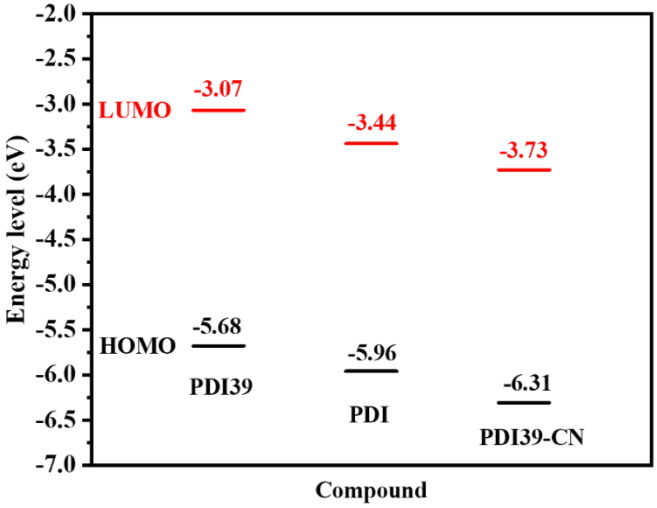

Figure S5. HOMO and LUMO energy levels of **PDI39**, **PDI** and **PDI39-CN** based on DFT calculation at b3lyp/6-31g** level.

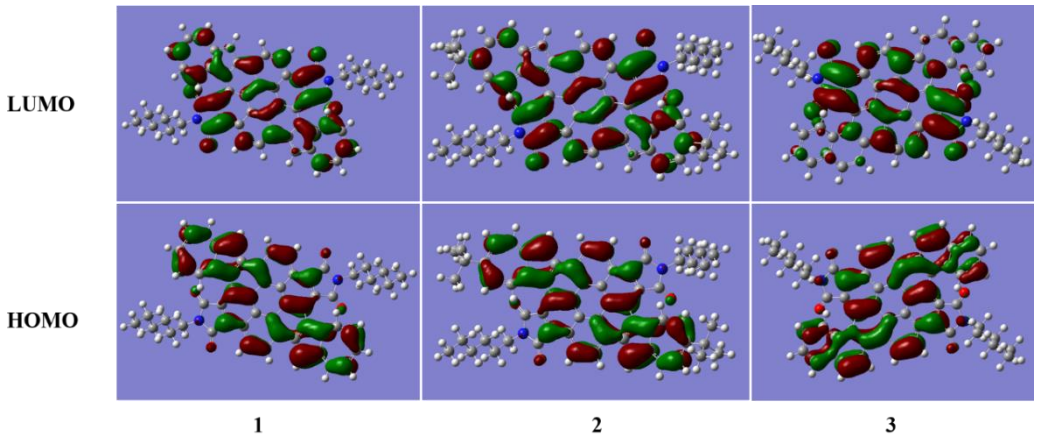

Figure S6. Frontier orbitals of **1**, **2** and **3** based on DFT calculation at b3lyp/6-31g** level.

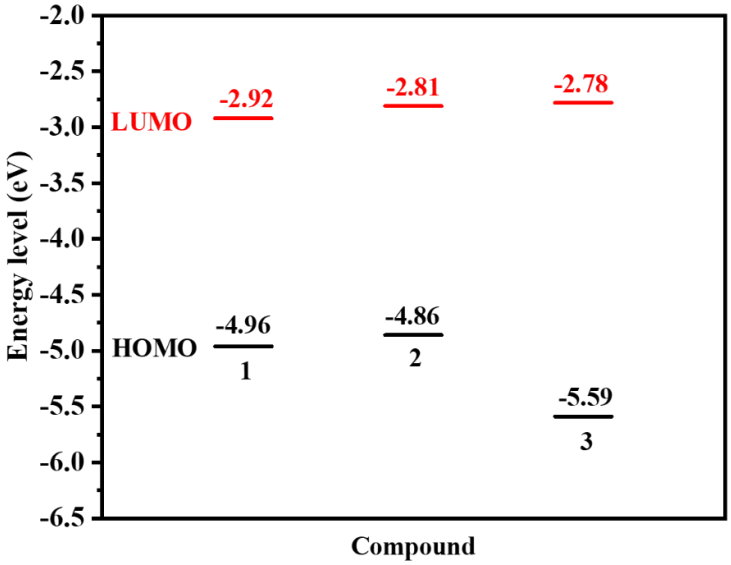

Figure S7. HOMO and LUMO energy levels of **1**, **2** and **3** based on DFT calculation at b3lyp/6-31g** level.

6. Calculations on conformation transformation

For the helical structure isomerization process and transfer barrier study, all calculations were performed with the Gaussian 09 program.[S7] Geometry optimizations of all stationary points were performed with the M06-2X functional.[S8] The 6-31G(d)[S9] basis set was applied for all elements in the molecule. Frequency calculations at the same level were performed to confirm each stationary point to be a minimum structure.

S7. Gaussian 09, Revision D.01, Frisch, M. J.; Trucks, G. W.; Schlegel, H. B.; Scuseria, G. E.; Robb, M. A.; Cheeseman, J. R.; Scalmani, G.; Barone, V.; Mennucci, B.; Petersson, G. A.; Nakatsuji, H.; Caricato, M.; Li, X.; Hratchian, H. P.; Izmaylov, A. F.; Bloino, J.; Zheng, G.; Sonnenberg, J. L.; Hada, M.; Ehara, M.; Toyota, K.; Fukuda, R.; Hasegawa, J.; Ishida, M.; Nakajima, T.; Honda, Y.; Kitao, O.; Nakai, H.; Vreven, T.; Montgomery, Jr., J. A.; Peralta, J. E.; Ogliaro, F.; Bearpark, M.; Heyd, J. J.; Brothers, E.; Kudin, K. N.; Staroverov, V. N.; Keith, T.; Kobayashi, R.; Normand, J.; Raghavachari, K.; Rendell, A.; Burant, J. C.; Iyengar, S. S.; Tomasi, J.; Cossi, M.; Rega, N.; Millam, J. M.; Klene, M.; Knox, J. E.; Cross, J. B.; Bakken, V.; Adamo, C.; Jaramillo, J.; Gomperts, R.; Stratmann, R. E.; Yazyev, O.; Austin, A. J.; Cammi, R.; Pomelli, C.; Ochterski, J. W.; Martin, R. L.; Morokuma, K.; Zakrzewski, V. G.; Voth, G. A.; Salvador, P.; Dannenberg, J. J.; Dapprich, S.; Daniels, A. D.; Farkas, O.; Foresman, J. B.; Ortiz, J. V.; Cioslowski, J.; Fox, D. J. Gaussian, Inc., Wallingford CT, 2013.

S8. (a) Zhao, Y.; Truhlar, D. G. *Acc. Chem. Res*. 2008, ***41***, 157. (b) Zhao, Y.; Truhlar, D. G. *Theor. Chem. Acc*. 2008, ***120***, 215.

S9. For the 6-31G(d) basis set, see: (a) Ditchfield, R.; Hehre, W. J.; Pople, J. A. *J. Chem. Phys.* 1971, ***54***, 724. (b) Hehre, W. J.; Ditchfield, R.; Pople, J. A. *J. Chem. Phys.* 1972, ***56***, 2257. (c) Hariharan, P. C.; Pople, J. A. *Theor. Chim. Acta* 1973, ***28***, 213. (d) Dill, J. D.; Pople, J. A. *J. Chem. Phys.* 1975, ***62***, 2921. (e) Francl, M. M.; Pietro, W. J.; Hehre, W. J.; Binkley, J. S.; Gordon, M. S.; DeFrees, D. J.; Pople, J. A. *J. Chem. Phys.* 1982, ***77***, 3654. (f) Hehre, W. J.; Radom, L.; Schleyer, P. v. R.; Pople, J. A. Ab Initio Molecular Orbital Theory; Wiley: New York, 1986.

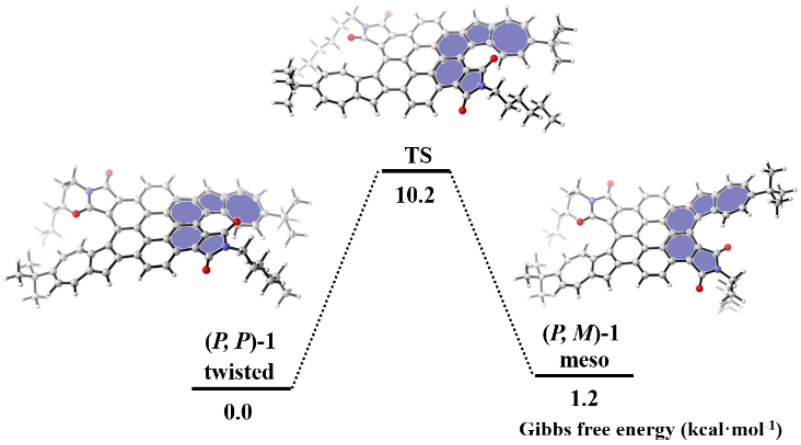

Figure S8. Gibbs free energy of the conformation transformation barrier of **2**.

7. Photophysical and electrochemical properties of 1-3

7.1 UV-Vis-NIR spectra of 1

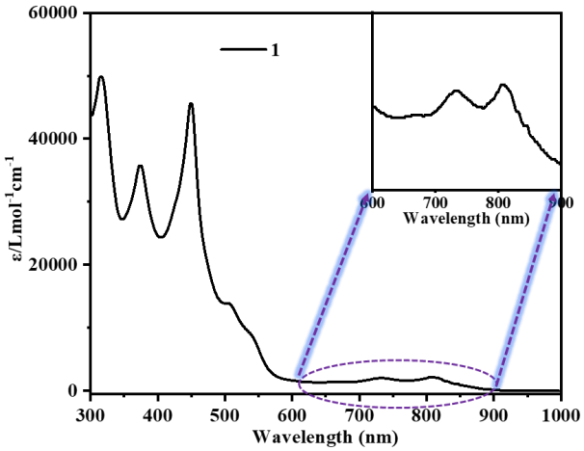

Figure S9. Absorption spectra of **1** in $CHCl_3$ solution (10^{-5} mol/L).

7.2 Cyclic voltammograms

Cyclic voltametric measurements were carried out in a three-electrode cell by using glassy carbon as the working electrode, a Pt wire as auxiliary electrode, an Ag/AgCl (saturated KCl) as reference electrode and n-Bu_4NPF_6 (0.1 mol/L in anhydrous dichloromethane) as the supporting electrolyte at a scan rate of 100 mV s^{-1}. For calibration, the redox potential of ferrocene/ferrocenium (Fc/Fc^+) was measured under the same conditions or as internal standard.

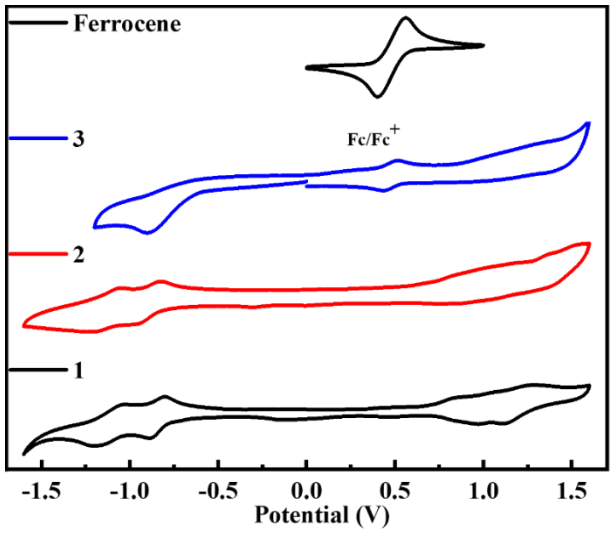

Figure S10. Cyclic voltammograms (CV) of compounds **1**, **2** and **3** in anhydrous dichloromethane with ferrocene/ferrocenium (Fc/Fc^+) as external standard at room temperature.

Table S4. Photophysical and electrochemical data of **1-3**.

Comp.	$\lambda_{abs}^{Solution}$ (nm)[a]	ε ($M^{-1}cm^{-1}$)[b]	E_{red}^{onset} (eV)[c]	E_{ox}^{onset} (eV)[c]	HOMO (eV)[d]	LUMO (eV)[e]	E_g(eV)[f]
1	810	2177	-0.74	0.70	-5.07	-3.63	1.44
	737	2016					
	451	45564					
2	796	4916	-0.78	0.67	-5.11	-3.66	1.45
	721	4375					
	456	105083					
3	533	17655	-0.63	0.92	-5.25	-3.70	1.55
	499	20484					
	392	84185					

[a] Absorption wavelength in $CHCl_3$ (10^{-5} mol/L); [b] Molar extinction coefficient at corresponding absorption peaks; [c] Cyclic voltammograms of anhydrous dichloromethane solution of **1-3** at a scan rate of 100 mVs^{-1}. Glassy carbon was used as working electrode and Pt wire was used as counter electrode and Ag/AgCl (saturated KCl) as reference electrode; n-Bu_4NPF_6 (0.1 M) in CH_2Cl_2 as supporting electrolyte. For calibration, the redox potential of ferrocene/ferrocenium (Fc/Fc^+) was measured under the same conditions; [d] HOMO energy calculated from $E_{HOMO} = -(4.80 + E_{ox}^{onset})$ eV; (e) LUMO energy levels calculated from $E_{LUMO} = -(4.80 + E_{red}^{onset})$ eV; (f) $E_g = E_{LUMO} - E_{HOMO}$

8. Single crystal X-ray diffraction analysis

8.1 XRD analysis of PDI39-CN

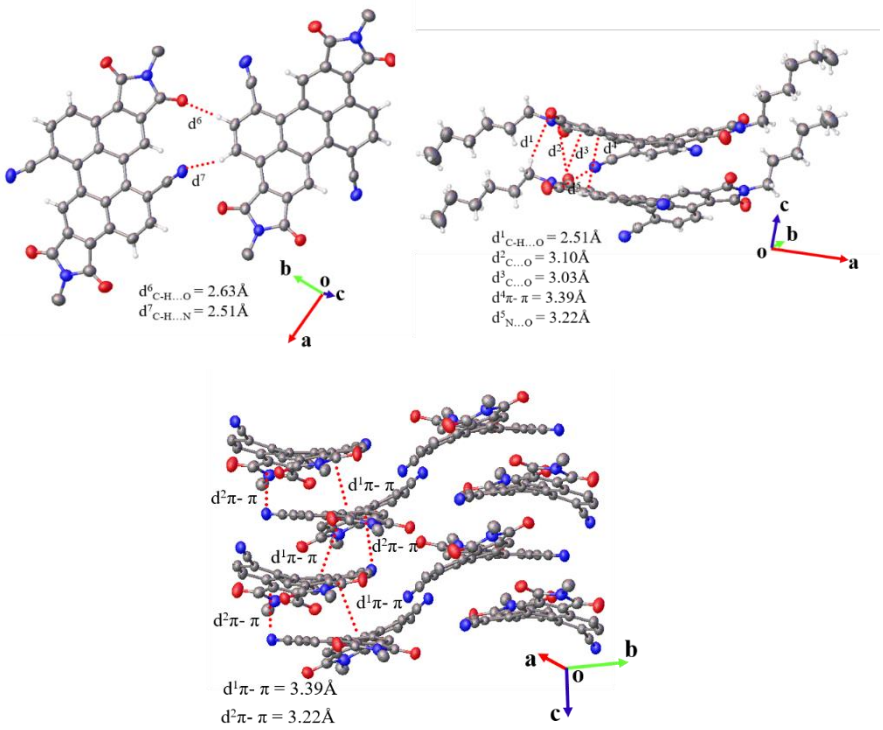

Figure S11. The crystal structure of **PDI39-CN** and the intermolecular interaction and packing within single crystal of **PDI39-CN**. Alkyl was omitted for clarity and displacement ellipsoids were drawn at 50% probability level.

8.2 XRD analysis of 2

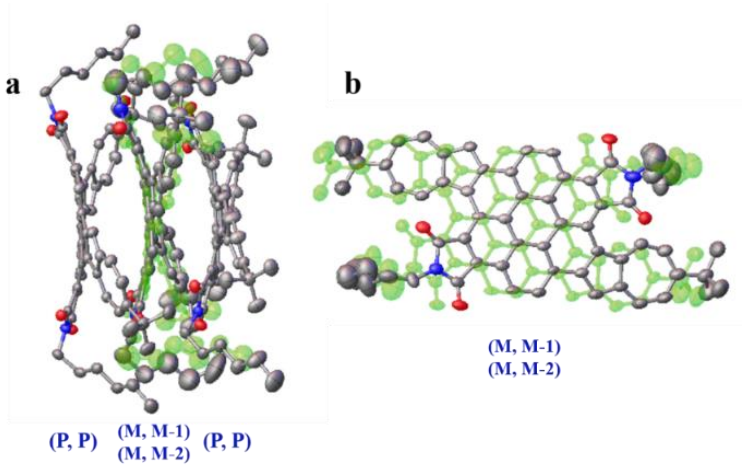

Figure S12. (a) Crystal packing of **2** in a unit cell (side view); (b) two conformers of (*M, M*) configurations (top view). Hydrogen atoms and alkyl chains were omitted for clarity and displacement ellipsoids were drawn at 50% probability level.

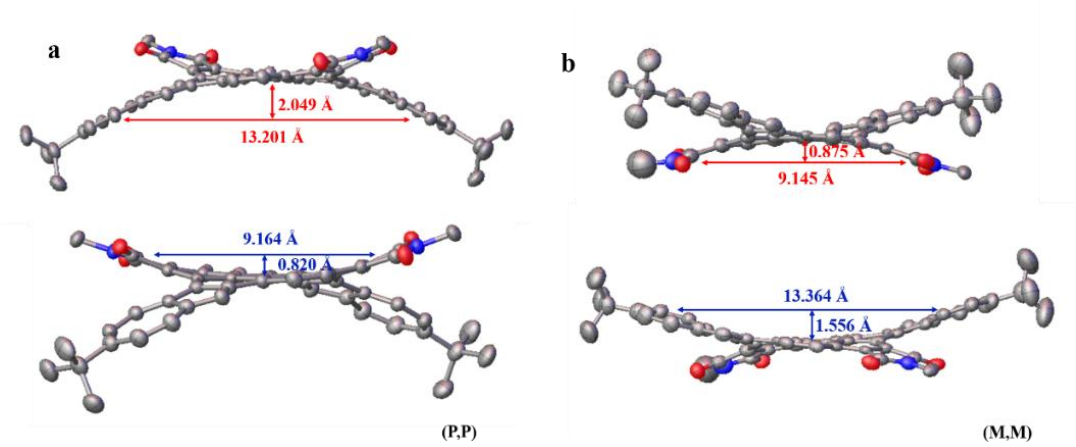

Figure S13. The Width and depth of the saddle-shaped curvature for (*P, P*) (a) and (*M, M*) (b). Hydrogen atoms and alkyl chains were omitted for clarity and displacement ellipsoids were drawn at 50% probability level.

Table S5. Selected C-C bond lengths of **2**.

Number	Atom	Atom	Bond Length (Å)
1	C3	C4	1.376 (4)
2	C4	C5	1.421 (4)
3	C5	C6	1.434 (4)
4	C6	C7	1.432 (4)
5	C7	C8	1.422 (4)
6	C8	C3	1.412 (4)
7	C5	C12	1.436 (4)
8	C12	C11	1.401 (4)
9	C11	C10	1.428 (4)
10	C10	C9	1.409 (4)
11	C9	C6	1.434 (4)
12	C11	C15	1.421 (4)
13	C15	C16	1.379 (4)
14	C16	C17	1.411(4)
15	C17	C18	1.363(4)
16	C18	C19	1.405(5)
17	C19	C20	1.381 (4)
18	C20	C21	1.426 (4)
19	C21	C22	1.367 (4)
20	C22	C12	1.453 (4)
21	C22	C16	1.475 (4)
22	C10	C13	1.405 (4)
23	C13	C14	1.358 (4)
24	C14	C8	1.409 (4)
25	C7	C9	1.436 (4)

Table S6. Crystallographic data of **PDI39**.

Identification code	**PDI39**
CCDC deposition NO.	2003562
Empirical formula	$C_{36}H_{34}N_2O_4$
Formula weight	558.65
Temperature/K	169.99(14)
Crystal system	triclinic
Space group	P-1
a/Å	10.8776(7)
b/Å	14.0655(13)
c/Å	18.9337(13)
α/°	95.710(7)
β/°	103.580(6)
γ/°	93.738(6)
Volume/Å^3	2790.1(4)
Z	4
ρ_{calc}g/cm^3	1.330
μ/mm^{-1}	0.691
F(000)	1184.0
Crystal size/mm^3	0.2× 0.1 × 0.02
Radiation	CuKα (λ = 1.54184)
2Θ range for data collection/°	4.836 to 151.742
Index ranges	-12 ≤ h ≤ 13, -17≤ k ≤ 17, -23 ≤ l ≤ 23
Reflections collected	29717
Independent reflections	10852 [R_{int} = 0.0864, R_{sigma} = 0.0894]
Data/restraints/parameters	10852/329/846
Goodness-of-fit on F^2	1.549
Final R indexes [I>=2σ (I)]	R_1 = 0.1362, wR_2 = 0.3000
Final R indexes [all data]	R_1 = 0.1941, wR_2 = 0.3340
Largest diff. peak/hole / e Å^{-3}	1.14/-0.54

Table S7. Crystallographic data of **PDI39-CN**.

Identification code	**PDI39-CN**
CCDC deposition NO.	2094430
Empirical formula	$C_{38}H_{32}N_4O_4$
Formula weight	608.67
Temperature/K	169.99(15)
Crystal system	monoclinic
Space group	$P2_1/c$
a/Å	24.4426(10)
b/Å	17.7385(5)
c/Å	7.0866(2)
α/°	90
β/°	92.811(3)
γ/°	90
Volume/Å^3	3068.88(18)
Z	4
ρ_{calc}g/cm^3	1.317
μ/mm^{-1}	0.697
F(000)	1280.0
Crystal size/mm^3	0.15× 0.08 × 0.03
Radiation	CuKα (λ = 1.54184)
2Θ range for data collection/°	6.158 to 151.268
Index ranges	$-29 \leq h \leq 29$, $-19 \leq k \leq 22$, $-7 \leq l \leq 8$
Reflections collected	21056
Independent reflections	6065 [R_{int} = 0.0505, R_{sigma} = 0.0437]
Data/restraints/parameters	6065/6/447
Goodness-of-fit on F^2	1.040
Final R indexes [I>=2σ (I)]	R_1 = 0.0554, wR_2 = 0.1506
Final R indexes [all data]	R_1 = 0.0761, wR_2 = 0.1663
Largest diff. peak/hole / e Å^{-3}	0.23/-0.26

Table S8. Crystallographic data of **2**.

Identification code	**2**
CCDC deposition NO.	2074735
Empirical formula	$C_{96}H_{87}N_3O_6$
Formula weight	1378.68
Temperature/K	169.99(14)
Crystal system	monoclinic
Space group	C2/c
a/Å	40.9622(10)
b/Å	10.7321(2)
c/Å	39.9989(10)
α/°	90
β/°	114.469(3)
γ/°	90
Volume/Å^3	16004.6(7)
Z	8
ρ_{calc}g/cm^3	1.144
μ/mm^{-1}	0.551
F(000)	1184.0
Crystal size/mm^3	0.12× 0.1 × 0.05
Radiation	CuKα (λ = 1.54184)
2Θ range for data collection/°	4.74 to 151.188
Index ranges	-33 ≤ h ≤ 51, -13≤ k ≤ 13, -49 ≤ l ≤ 49
Reflections collected	58606
Independent reflections	15863 [R_{int} = 0.0822, R_{sigma} = 0.0724]
Data/restraints/parameters	15863/997/1277
Goodness-of-fit on F^2	1.027
Final R indexes [I>=2σ (I)]	R_1 = 0.0737, wR_2 = 0.1928
Final R indexes [all data]	R_1 = 0.1300, wR_2 = 0.2267
Largest diff. peak/hole / e Å^{-3}	0.65/-0.58

9. OFETs fabrication and characterization

9.1 OFETs fabrication conditions

Substrate processing

The substrates were first cleaned by sonication in acetone and water and immersed in Piranha solution (2:1 mixture of sulfuric acid and 30% hydrogen peroxide) for 30 min, followed by rinsing with deionized water and isopropyl alcohol for several times, and they were blow-dried with nitrogen. Then, the substrate was processed by UV ozone about 10 min. After that, the substrates were placed into a petri dish, and one drop of n-octadecyltrichlorosilane (OTS) was dropped into the middle of petri dish. The system was stored under vacuum at 125 ºC for 4 h to form an OTS self-assembled monolayer.[S10-11] After the substrate surfaces were modified with OTS, they were washed with n-hexane, $CHCl_3$ and isopropyl alcohol sequentially. These substrates were used directly for **1** and **PDI39-CN**. For **PDI39**, the substrates needed to submerge in *p*-Toluenethiol (MBT) to modify the gold electrodes with concentration of 1.8 mg/mL in acetonitrile overnight and then annealed at 70 ºC for 10 min to remove residual solvent.[S12]

Thin-films OFET fabrications for PDI39 and PDI39-CN.

Bottom gate bottom contact (BGBC) field-effect transistors were fabricated by slowly depositing **PDI39** or **PDI39-CN** on OTS-treated Si/SiO_2 substrate under high vacuum with an active layer thickness of 40 nm at the rate of 0.1~0.2 Å/s. The substrates' temperature was kept at 50 ºC, 80 ºC, and 100 ºC for **PDI39** and rt, 50 ºC, 80 ºC, and 100 ºC for **PDI39-CN**.

Thin-films OFET fabrications for 1.

Bottom gate bottom contact (BGBC) field-effect transistors were fabricated by spin-coating method as follows: **1** was dissolve in chloroform (3 mg/mL) and spin-coating on OTS-treated Si/SiO_2 substrate at 2000 rpm for 50 s. The substrates were annealed at rt, 60 ºC, 120 ºC, and 160 ºC for 10 minutes.

OFET measurement conditions

A heavily doped n-type Si wafer and a layer of dry oxidized SiO_2 (300 nm, with capacitance of 11.5 nF cm^{-2}) were used as a gate electrode and gate dielectric layer, respectively. The drain-source (D-S) gold contacts were fabricated by photo-lithography. Characteristics of the devices were determined in glove box using a Keithley 4200 SCS semiconductor parameter analyzer. The mobility of the OFETs in the saturation region was extracted from the following equation:

$I_{DS} = \mu C_i (V_{GS} - V_{Th})^2 \, W/2L$

Where I_{DS} is the current collected by drain electrode; L and W are the channel length and width, respectively; μ is the mobility of the device; C_i is the capacitance per unit area of the gate dielectric layer; V_{GS} is the gate voltage, and V_{Th} is the threshold voltage.

9.2 OFETs performance of PDI39

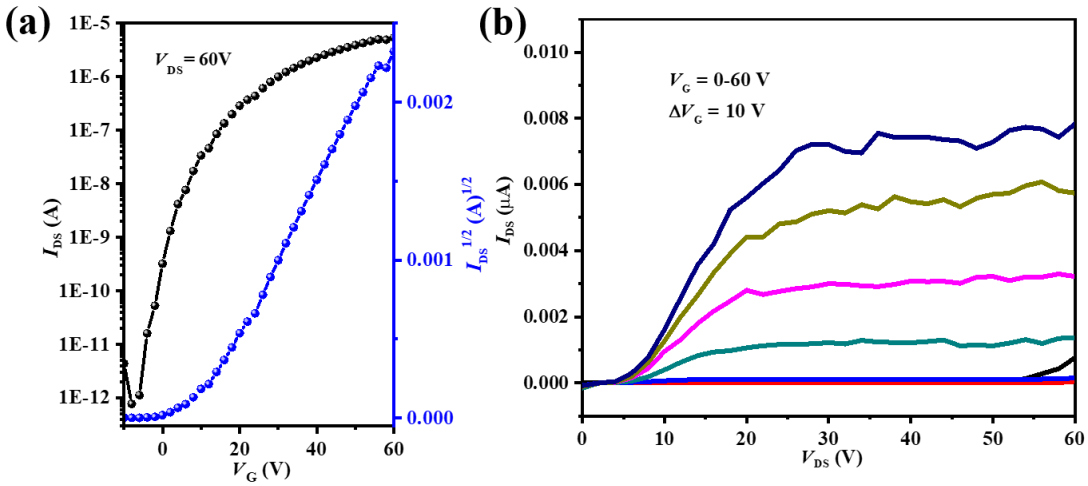

Figure S14. Typical transfer (a) and output (b) curves of deposited film of **PDI39**.

Table S9. The performance data of OFETs with **PDI39** at different substrate temperatures.

Comp.	T_{sub} (°C) [a]	μ/(cm^{2}V^{-1}s^{-1}) [max(ave)][b]	I_{on}/I_{off}[c]	V_{Th} (V)[d]
PDI39	50	0.0029(0.0012)	>10^6	25~27
	80	0.0016(0.0014)	>10^6	8~10
	100	3.5×10^{-4}(2.3×10^{-4})	>10^5	30~32

a. Substrate temperature; b. Electron mobility including maximum and average value; c. Current on/off ratio; d. threshold voltage. The average mobility was obtained based on more than 5 OFETs devices.

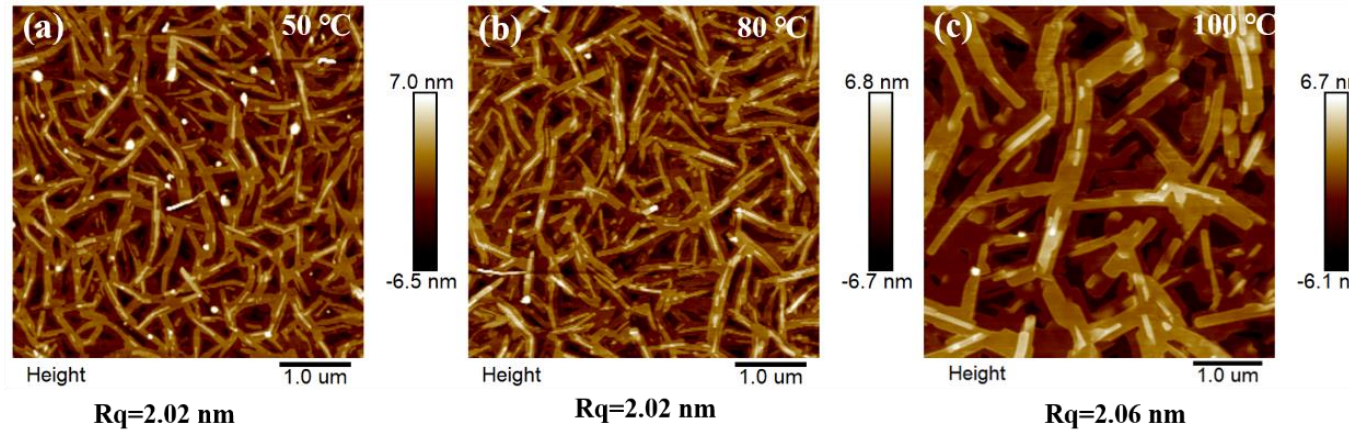

Figure S15. AFM height images of the deposited thin films of compound **PDI39** at different substrate temperatures.

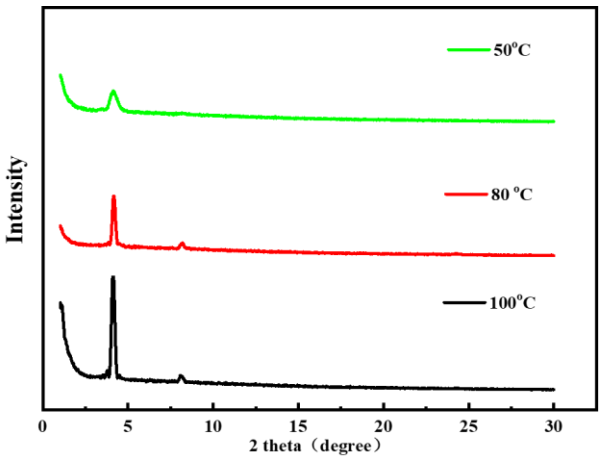

Figure S16. XRD patterns of the deposited thin films of compound **PDI39** at different substrate temperatures.

9.3 OFETs performance of PDI39-CN

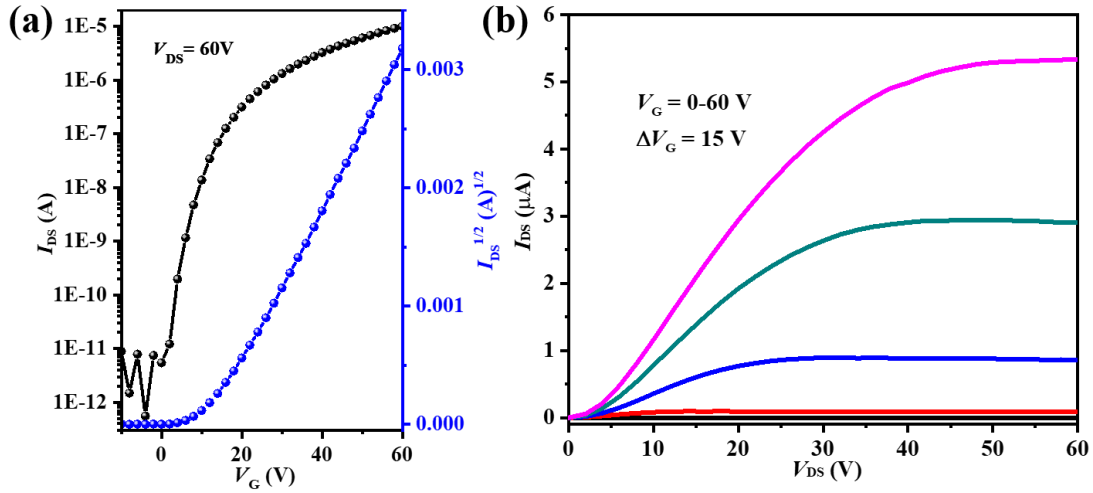

Figure S17. Typical transfer (a) and output curves (b) of deposited film of **PDI39-CN**.

Table S10. The performance data of OFETs with **PDI39-CN** at different substrate temperatures.

Comp.	T_{sub}/ °C [a]	μ/(cm^{2}V^{-1}s^{-1}) [max(ave)][b]	I_{on}/I_{off}[c]	V_{Th} (V)[d]
PDI39-CN	25	0.017(0.014) [0.018 (0.014)][e]	10^5~10^6 [10^5~10^6][e]	6-11 [16-24] [e]
	50	0.031(0.028)	10^5~10^6	11-15
	80	0.025(0.022)	10^5~10^6	10-15
	100	0.018(0.015)	10^5~10^6	5-8

a. Substrate temperature; b. Electron mobility including maximum and average value; c. Current on/off ratio; d. Threshold voltage; e. Mobility was obtained under air atmosphere. The average mobility was obtained based on more than 20 OFETs devices.

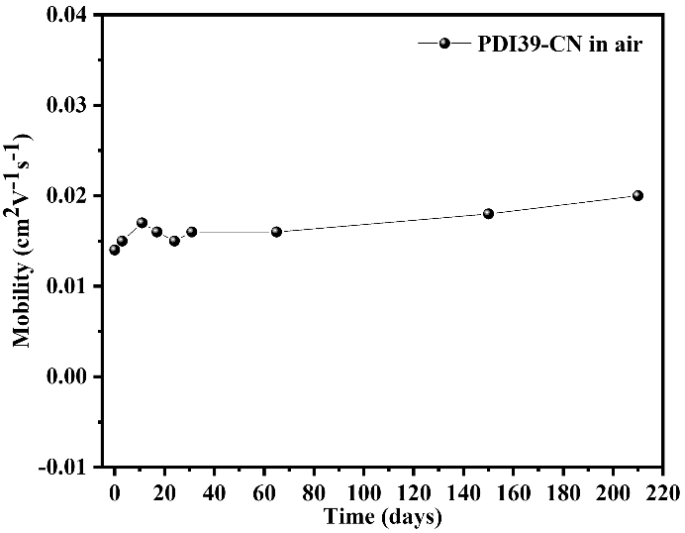

Figure S18. Average mobilities of **PDI39-CN** after storing the OFETs devices under air atmosphere for different time. The average mobility was obtained based on more than 20 OFETs devices. The temperature range was about 26-35 ºC and humidity was about 60%-90%.

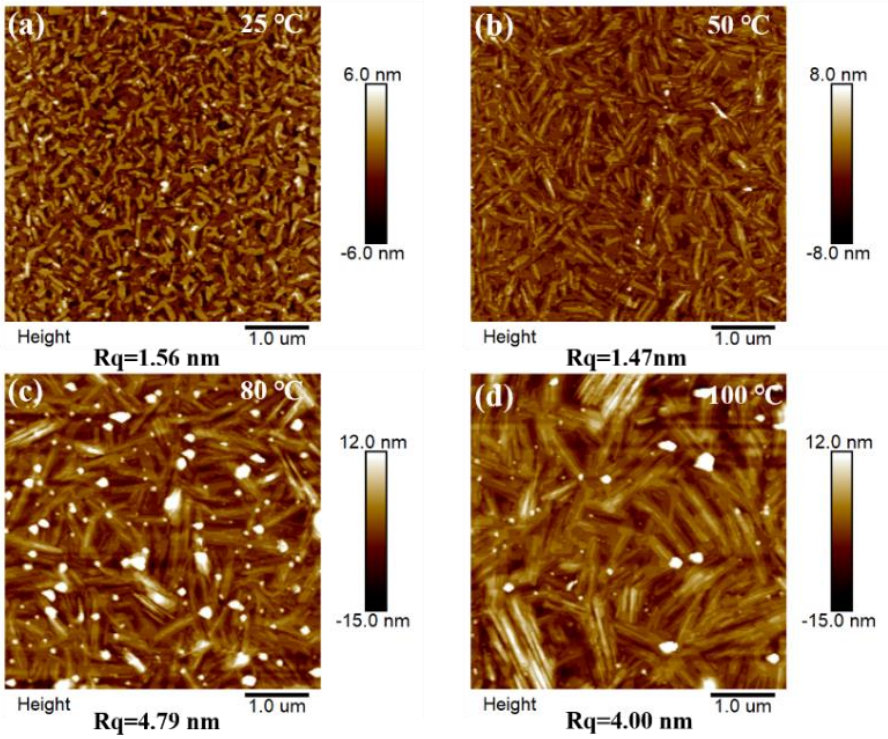

Figure S19. AFM height images of the deposited thin films of compound **PDI39-CN** at different substrate temperatures.

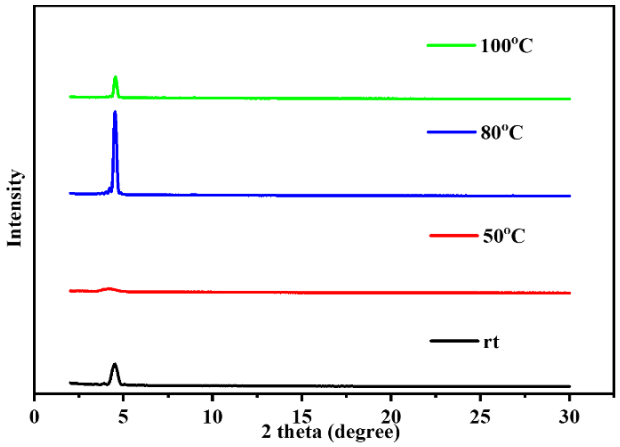

Figure S20. XRD patterns of the deposited thin films of compound **PDI39-CN** at different substrate temperatures.

9.4 OFETs performance of 1

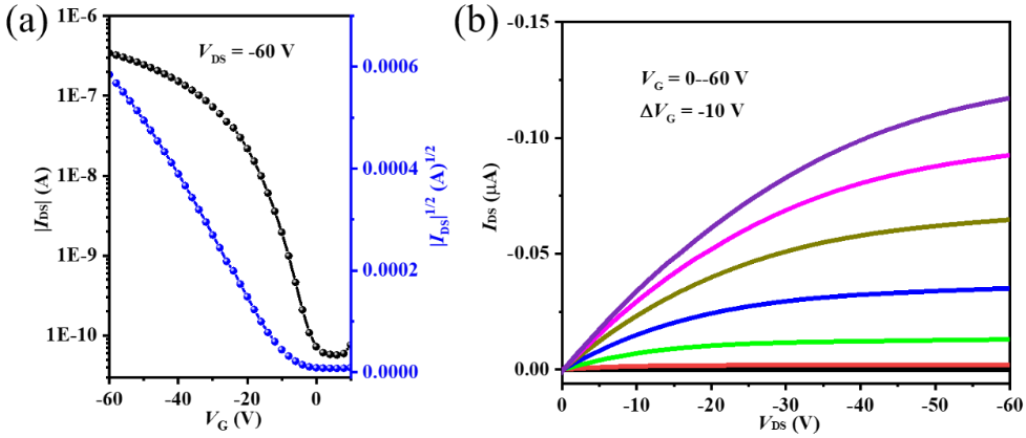

Figure S21. Typical transfer (a) and output (b) curves solution-processed film of **1**.

Table S11. The performance data of OFETs with **1** after annealing at different temperatures.

Comp.	T_{anneal}/ °C [a]	$\mu_h \times 10^4$(cm^{2}V^{-1}s^{-1}) [max(ave)][b]	I_{on}/I_{off} [c]	V_{Th}(V) [d]
1	25	1.0(0.6)	~10^4	-2~-5
	60	1.6(1.0)	~10^4	-1~-4
	120	1.3(0.8)	~10^4	-2~-6
	160	1.0(0.6)	~10^4	-2~-6

a. Annealing temperature under air; b. Hole mobility including maximum and average value; c. Current on/off ratio; d. Threshold voltage. The average mobility was obtained based on more than 20 OFETs devices.

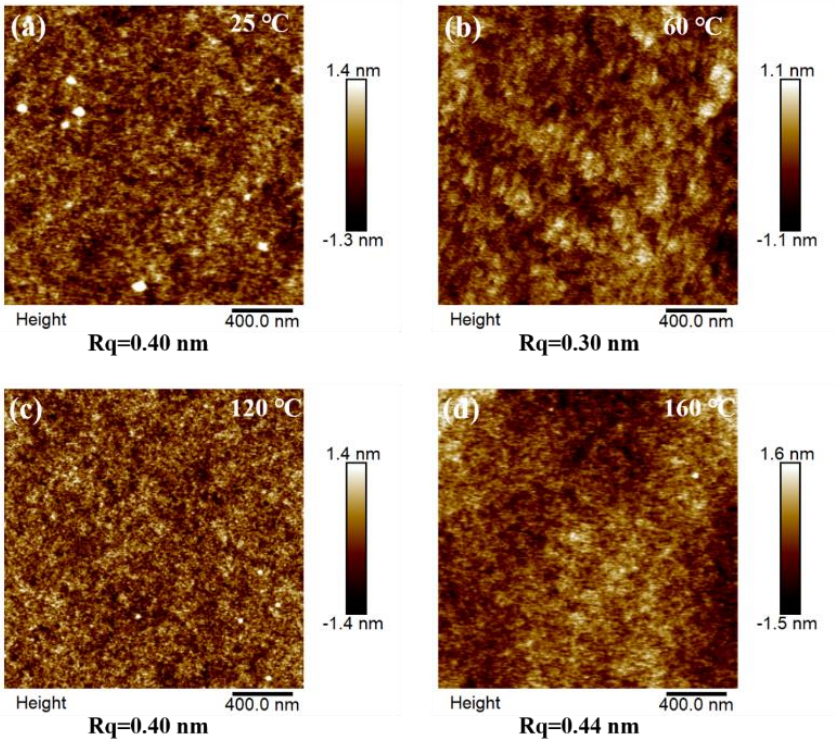

Figure S22. AFM height images of the thin films of compound **1** by spin coating.

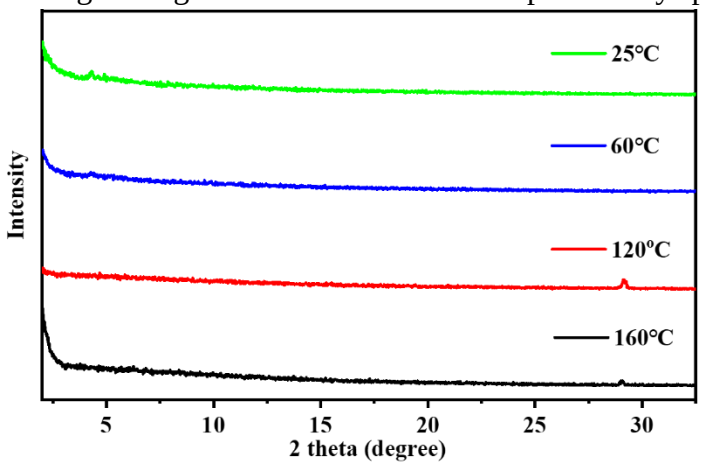

Figure S23. XRD patterns of the thin films of compound **1** by spin coating.

10 ^{1}H NMR and ^{13}C NMR spectra

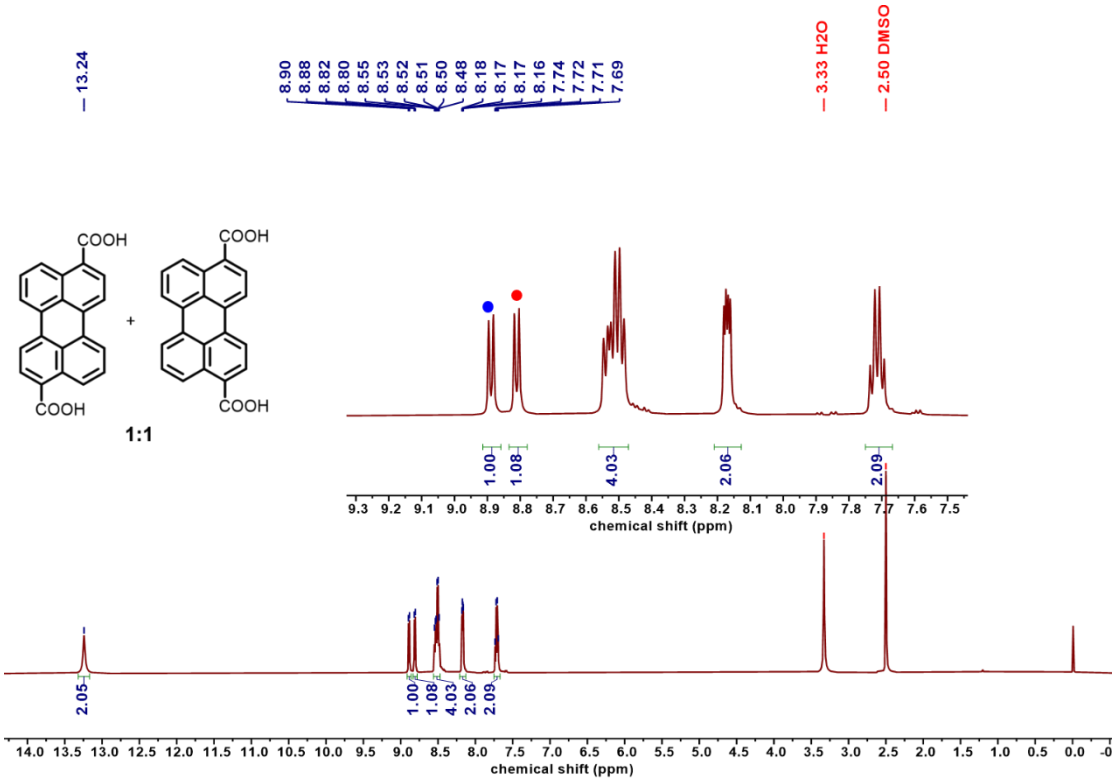

Figure S24. ^{1}H NMR spectrum of "compound" **4** (600 MHz, d_6-DMSO, 298 K).

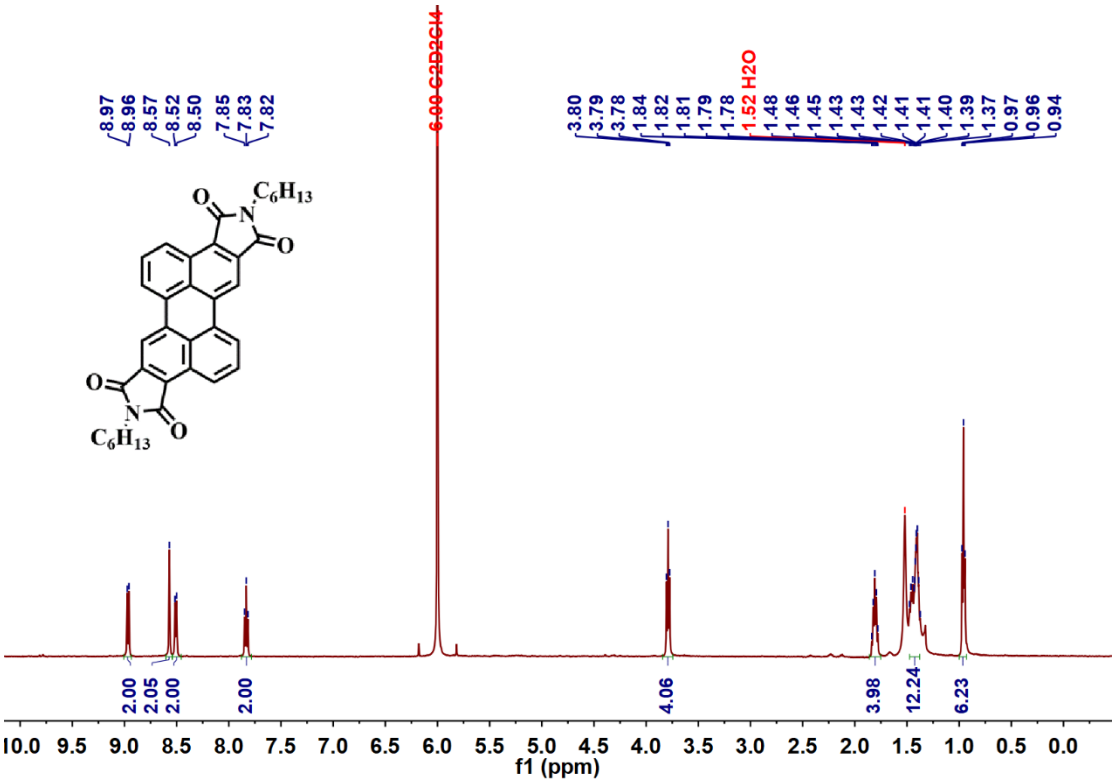

Figure S25. ^{1}H NMR spectrum of compound **PDI39** (500 MHz, $C_2D_2Cl_4$, 353.2 K).

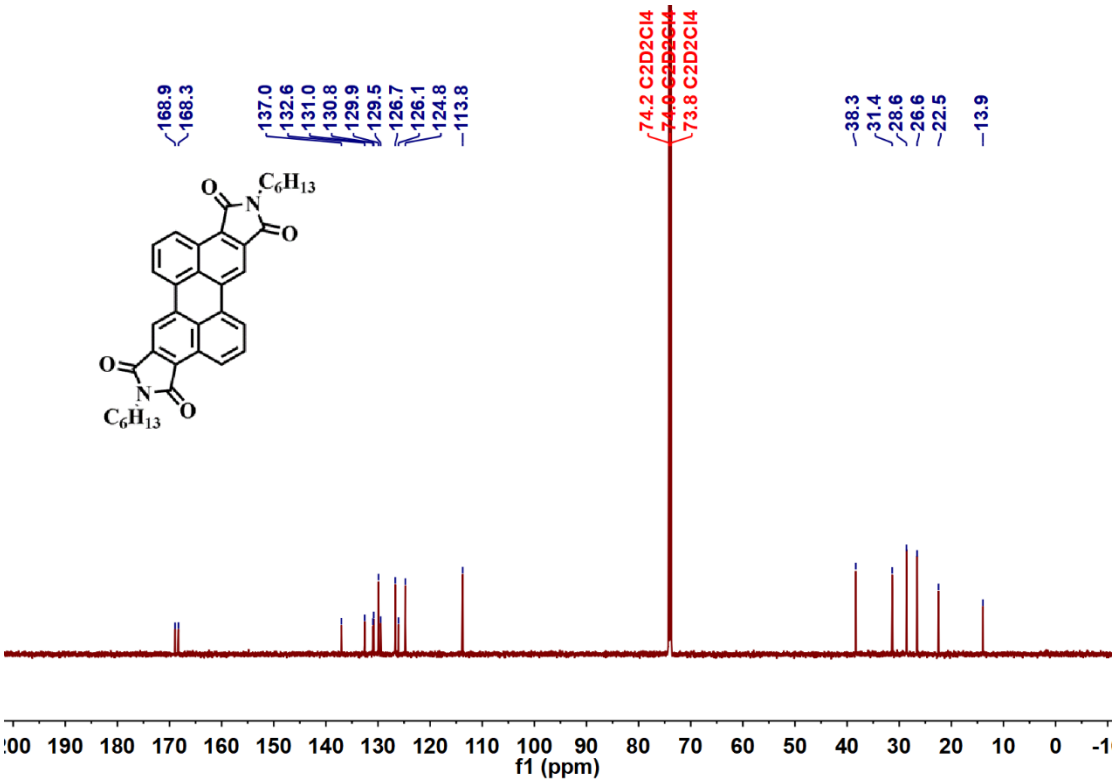

Figure S26. ^{13}C NMR spectrum of compound **PDI39** (125 MHz, $C_2D_2Cl_4$, 353.2 K).

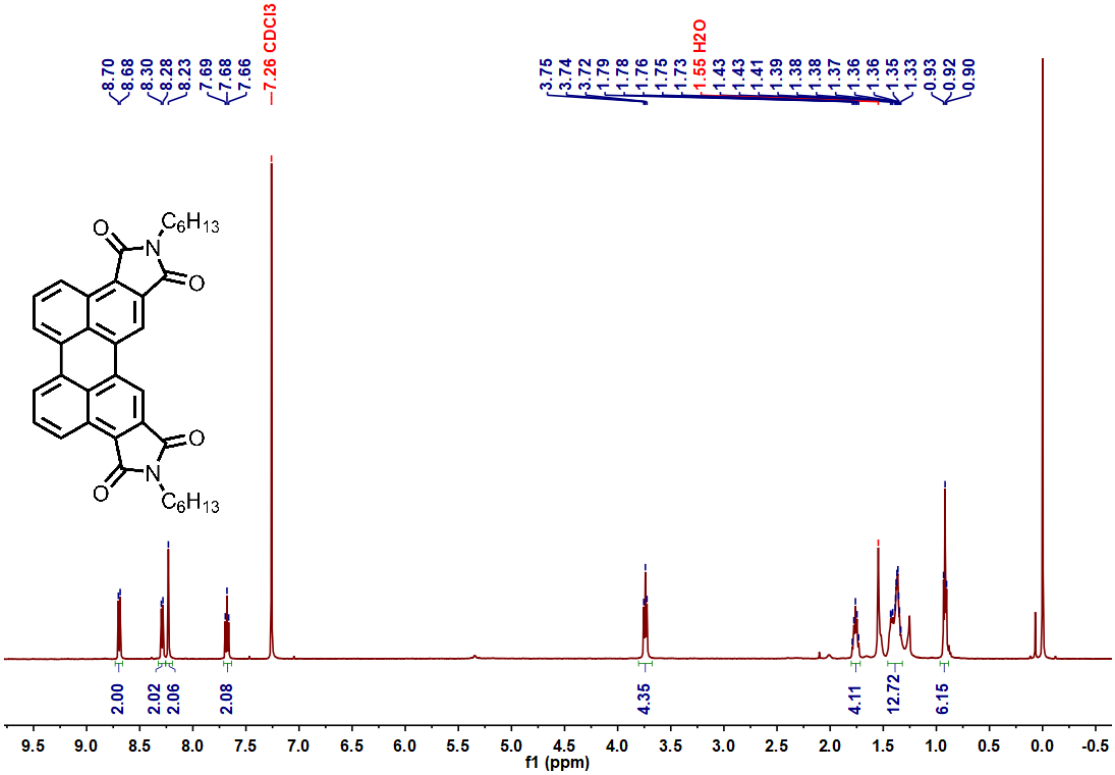

Figure S27. ^{1}H NMR spectrum of compound **PDI310** (500 MHz, $CDCl_3$, 298 K).

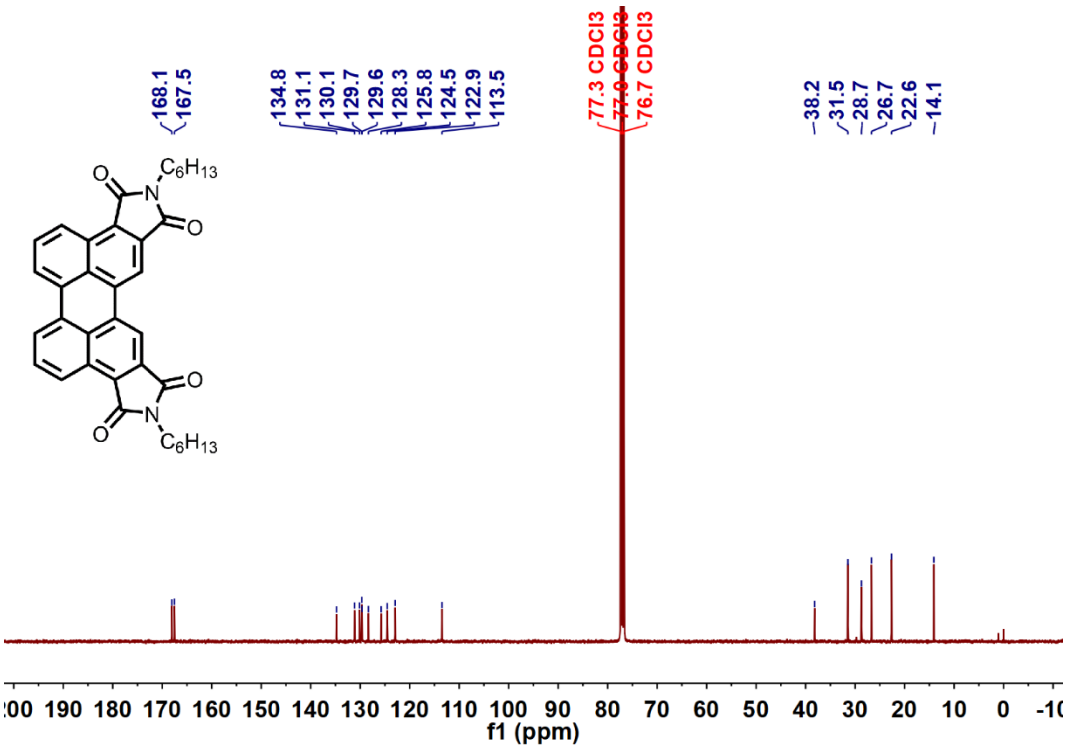

Figure S28. ^{13}C NMR spectrum of compound **PDI310** (100 MHz, $CDCl_3$, 298 K).

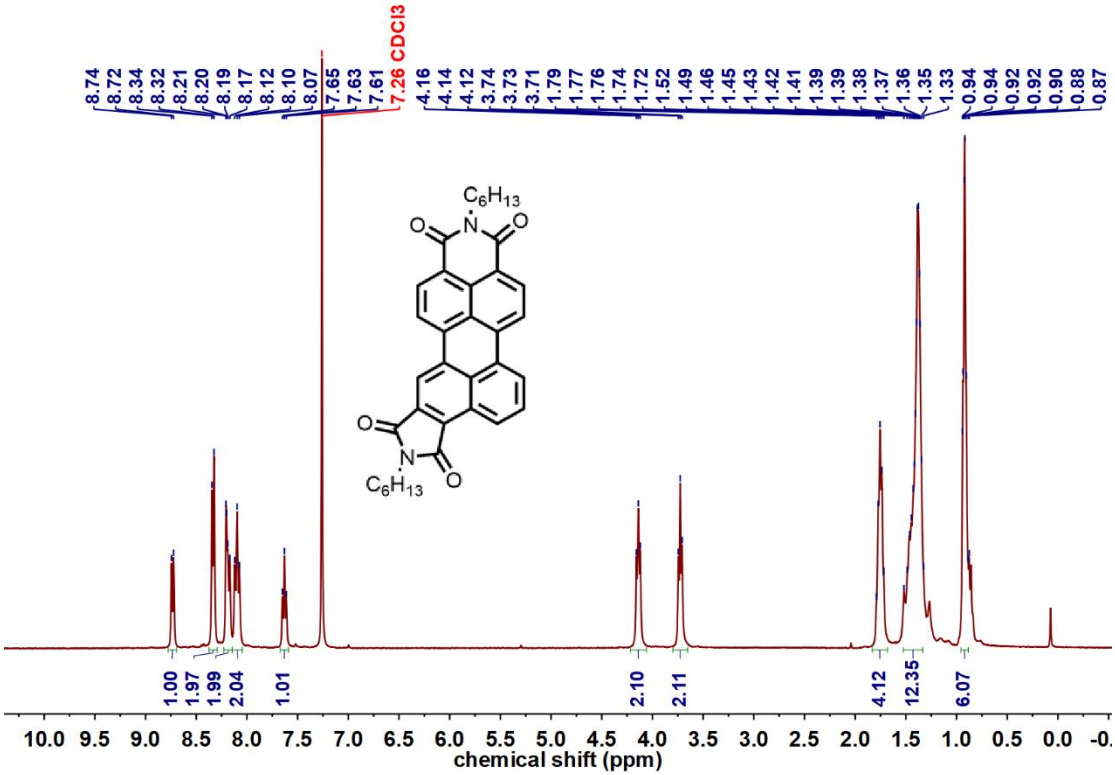

Figure S29. ^{1}H NMR spectrum of compound **PDI56** (400 MHz, $CDCl_3$, 298 K).

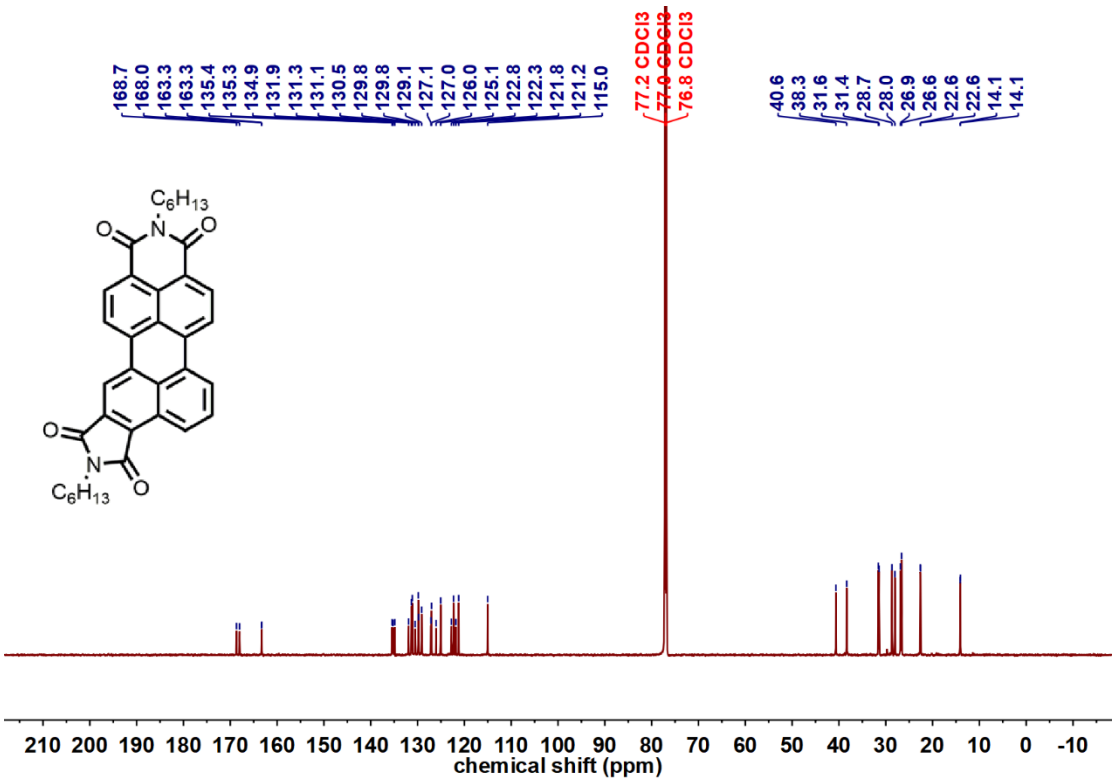

Figure S30. ^{1}H NMR spectrum of compound **PDI56** (176 MHz, $CDCl_3$, 298 K).

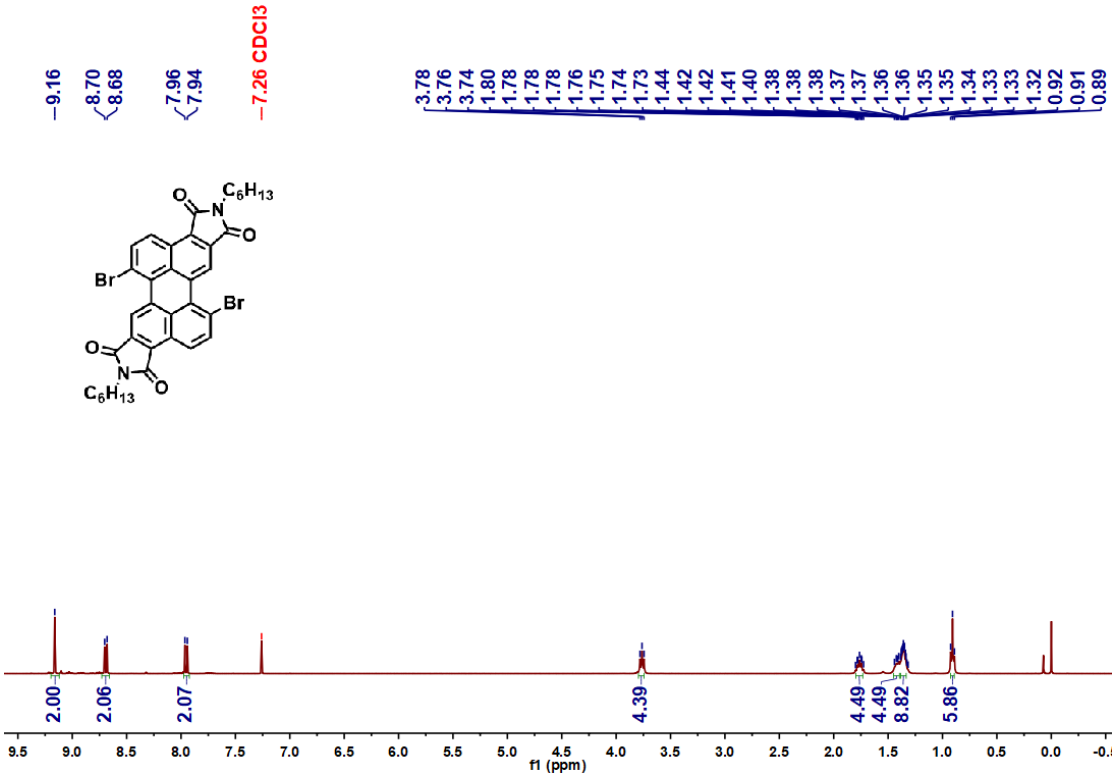

Figure S31. ^{1}H NMR spectrum of compound **PDI39-Br** (400 MHz, $CDCl_3$, 298 K).

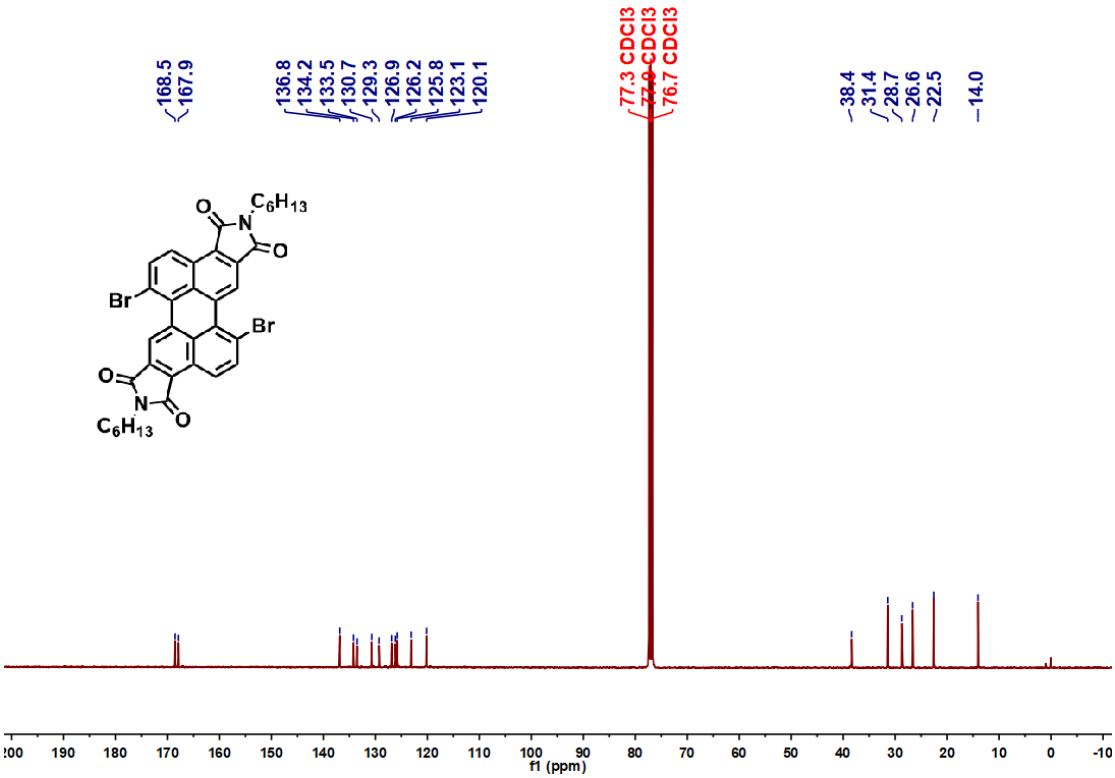

Figure S32. ^{13}C NMR spectrum of compound **PDI39-Br** (100 MHz, $CDCl_3$, 298 K).

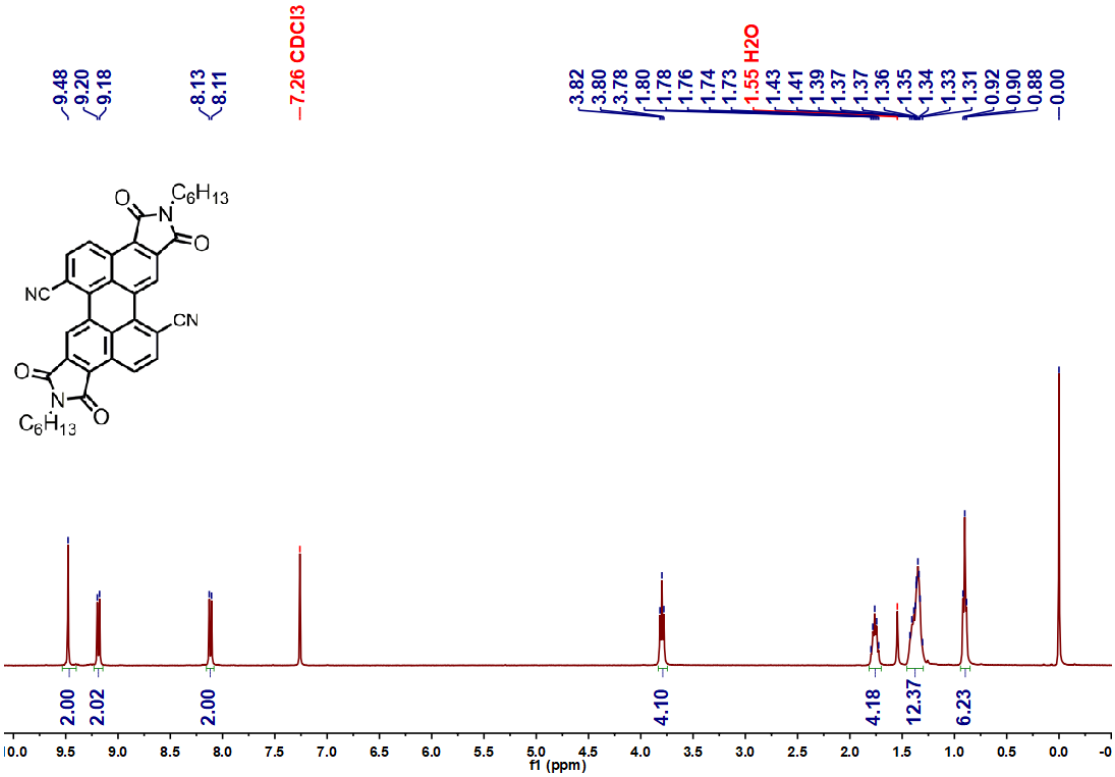

Figure S33. ^{1}H NMR spectrum of compound **PDI39-CN** (400 MHz, $CDCl_3$, 298 K).

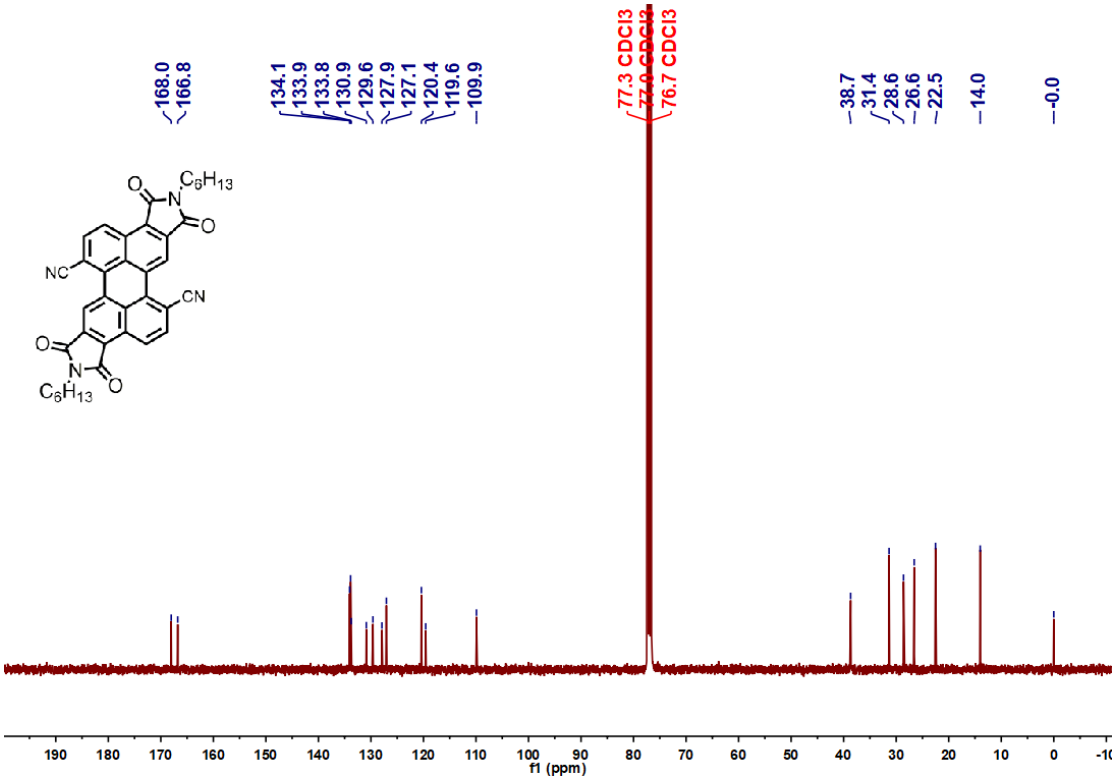

Figure S34. ^{13}C NMR spectrum of compound **PDI39-CN** (100 MHz, $CDCl_3$, 298 K).

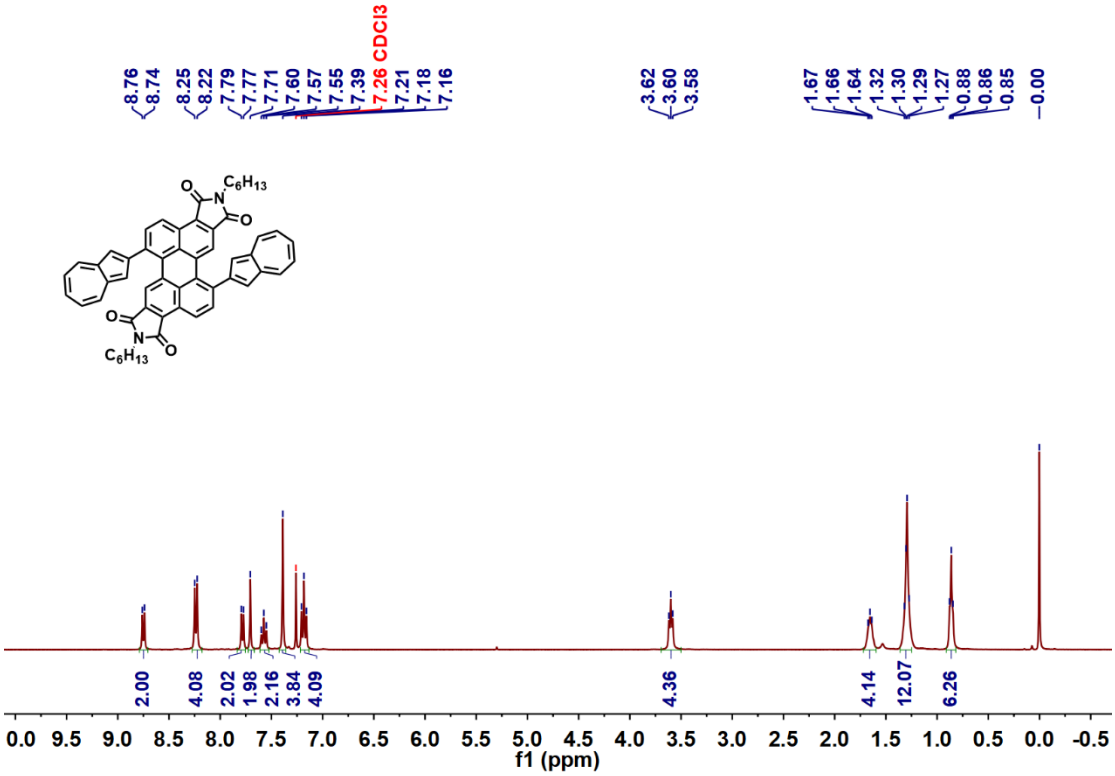

Figure S35. ^{1}H NMR spectrum of compound **8** (400 MHz, $CDCl_3$, 298 K).

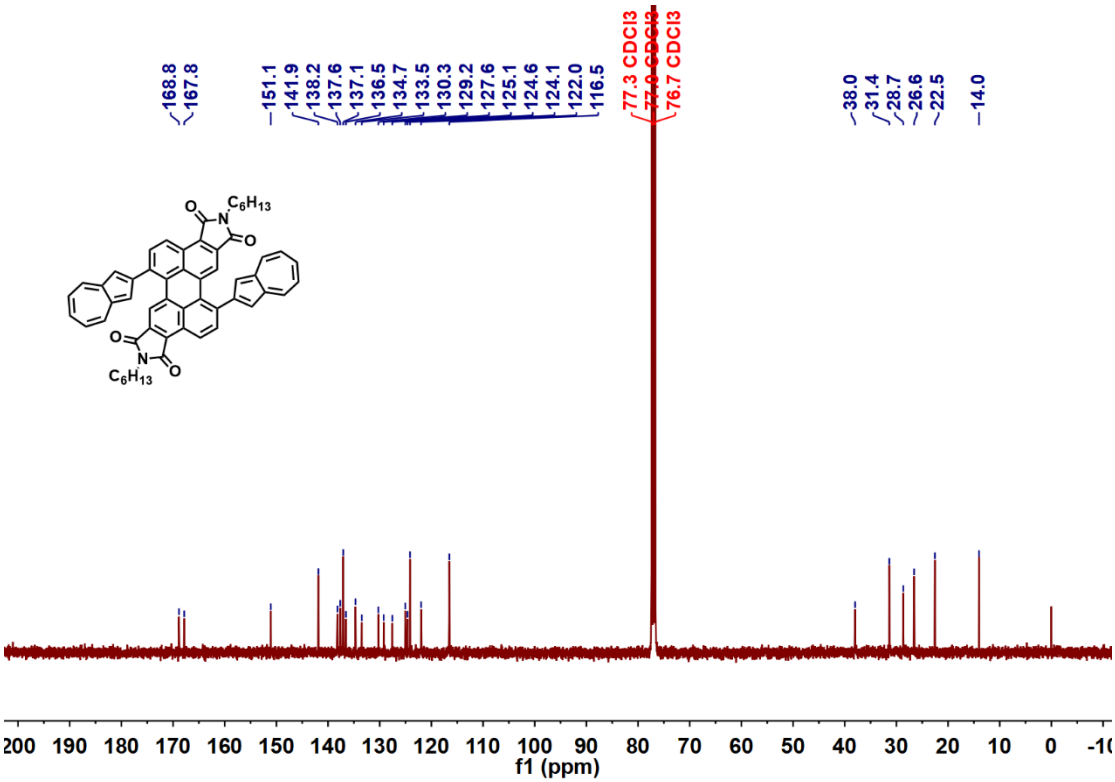

Figure S36. ^{13}C NMR spectrum of compound **8** (100 MHz, $CDCl_3$, 298 K).

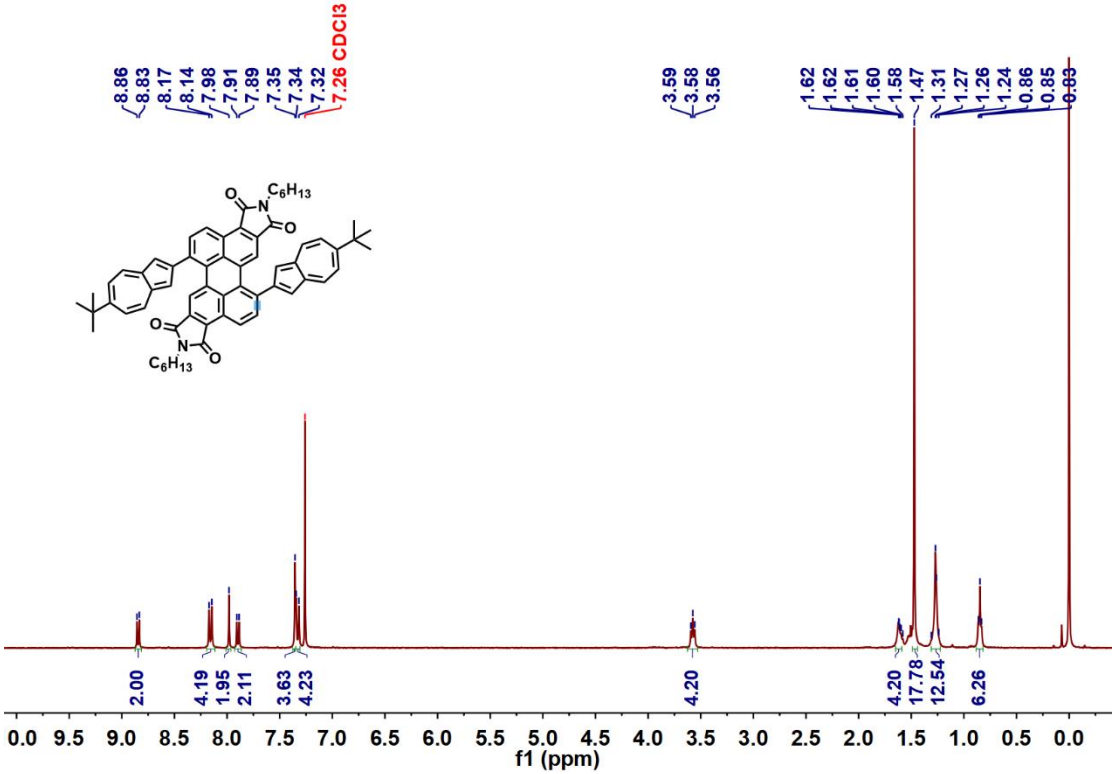

Figure S37. ^{1}H NMR spectrum of compound **9** (400 MHz, $CDCl_3$, 298 K).

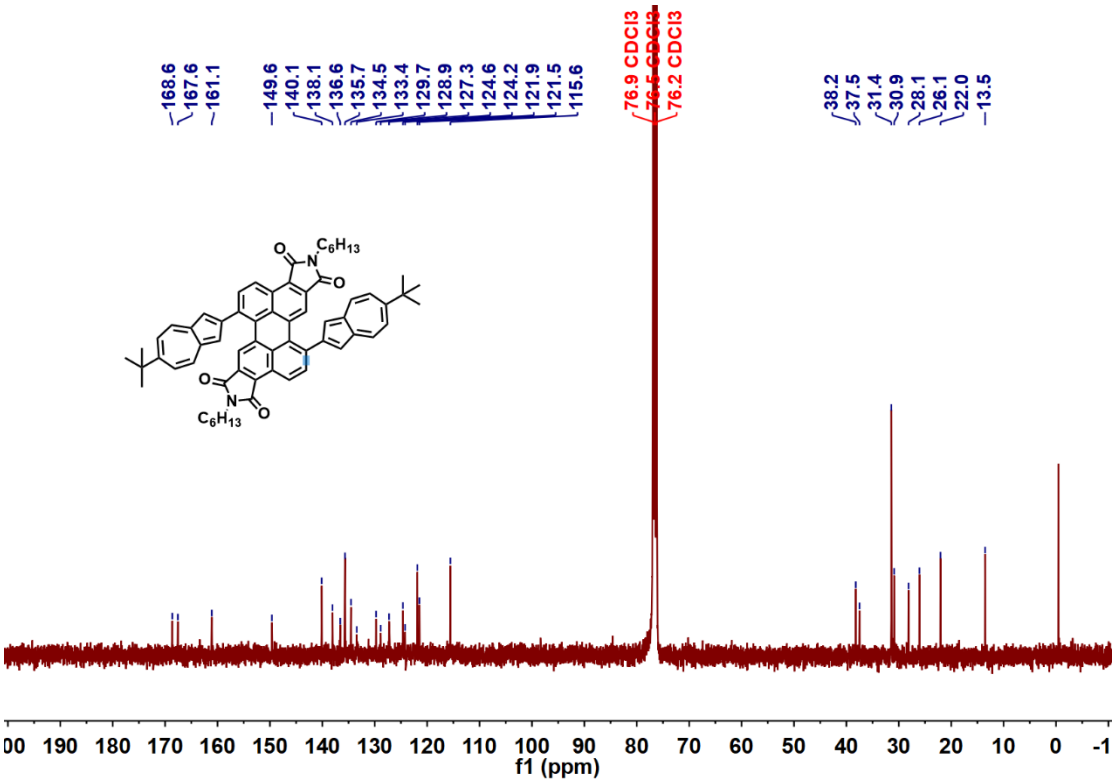

Figure S38. ^{13}C NMR spectrum of compound **9** (100 MHz, $CDCl_3$, 298 K).

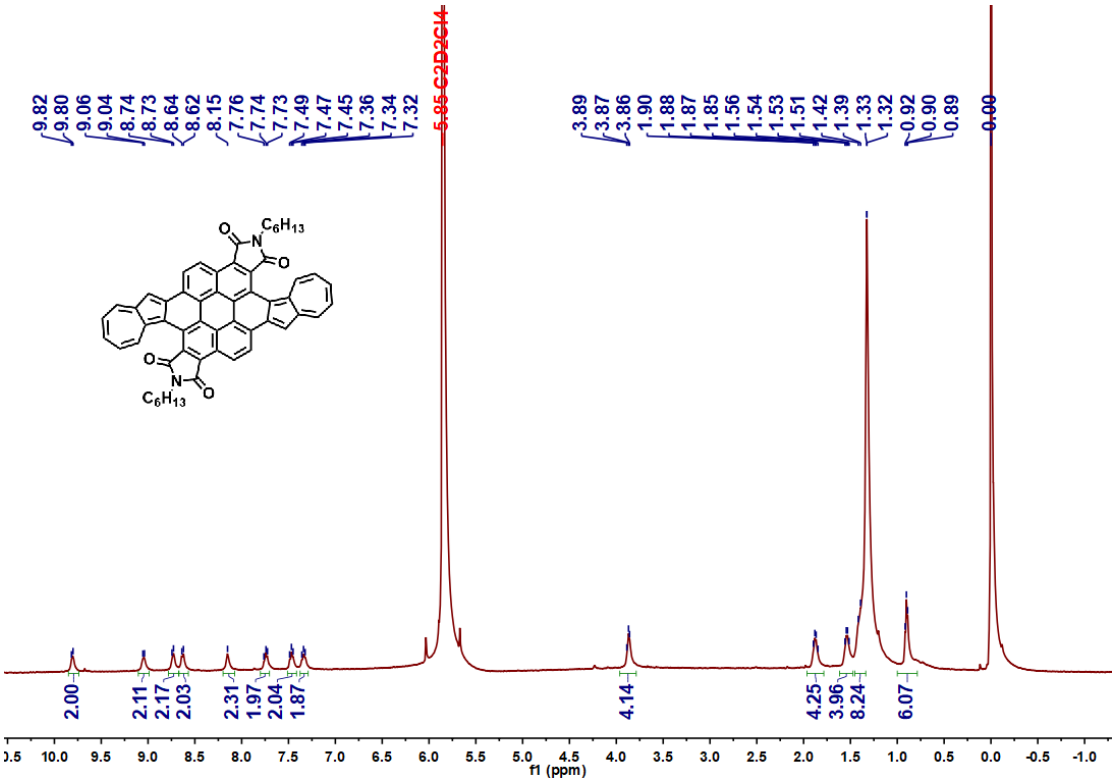

Figure S39. ^{1}H NMR spectrum of compound **1** (500 MHz, $C_2D_2Cl_4$, 373.2 K).

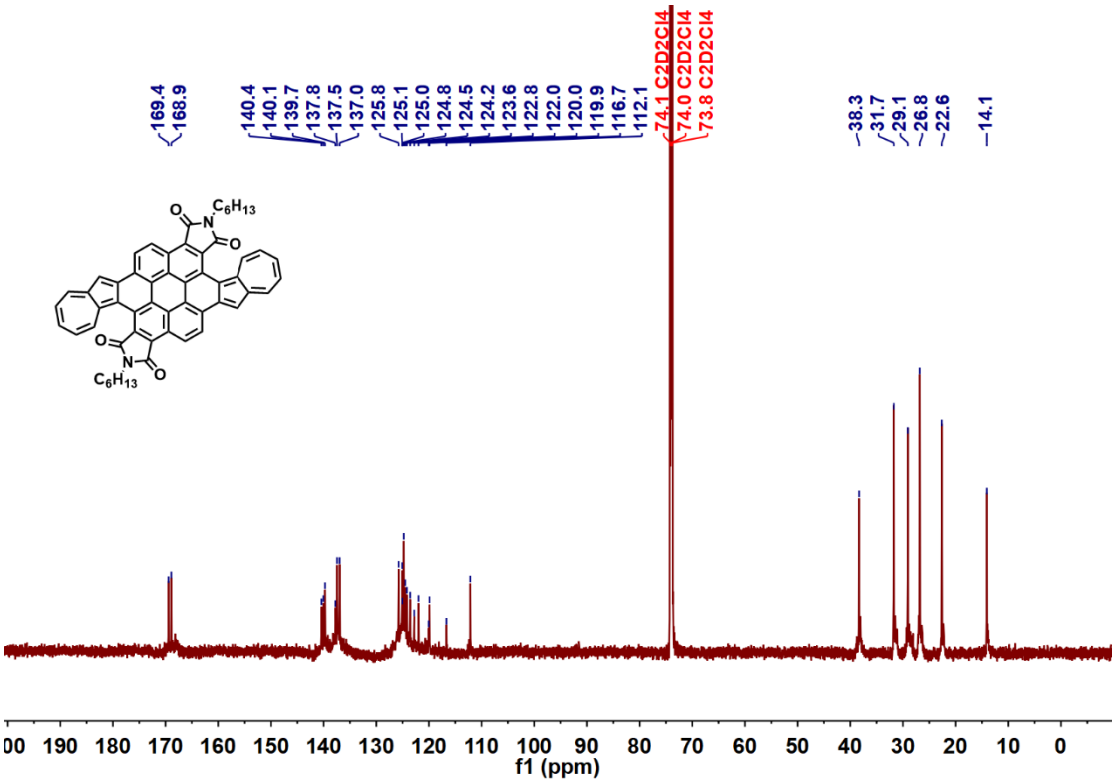

Figure S40. ^{13}C NMR spectrum of compound **1** (176 MHz, $C_2D_2Cl_4$, 373.2 K).

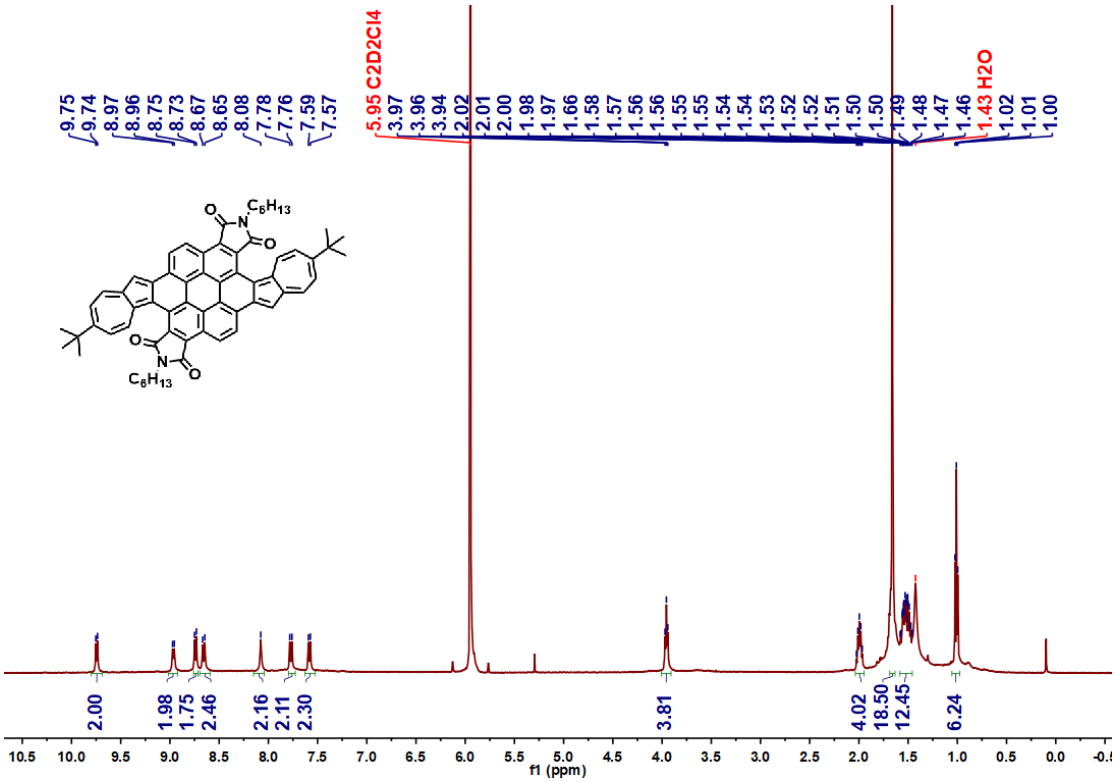

Figure S41. ^{1}H NMR spectrum of compound **2** (500 MHz, $C_2D_2Cl_4$, 373.2 K).

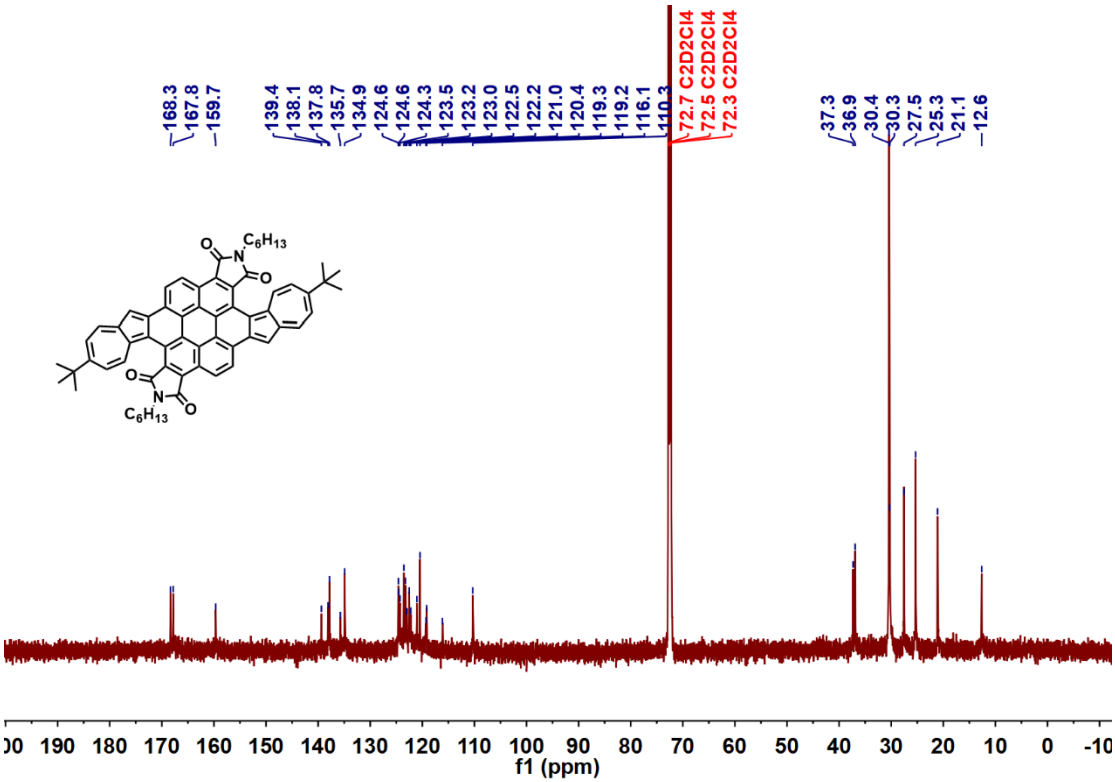

Figure S42. ^{13}C NMR spectrum of compound **2** (125 MHz, $C_2D_2Cl_4$, 373.2 K).

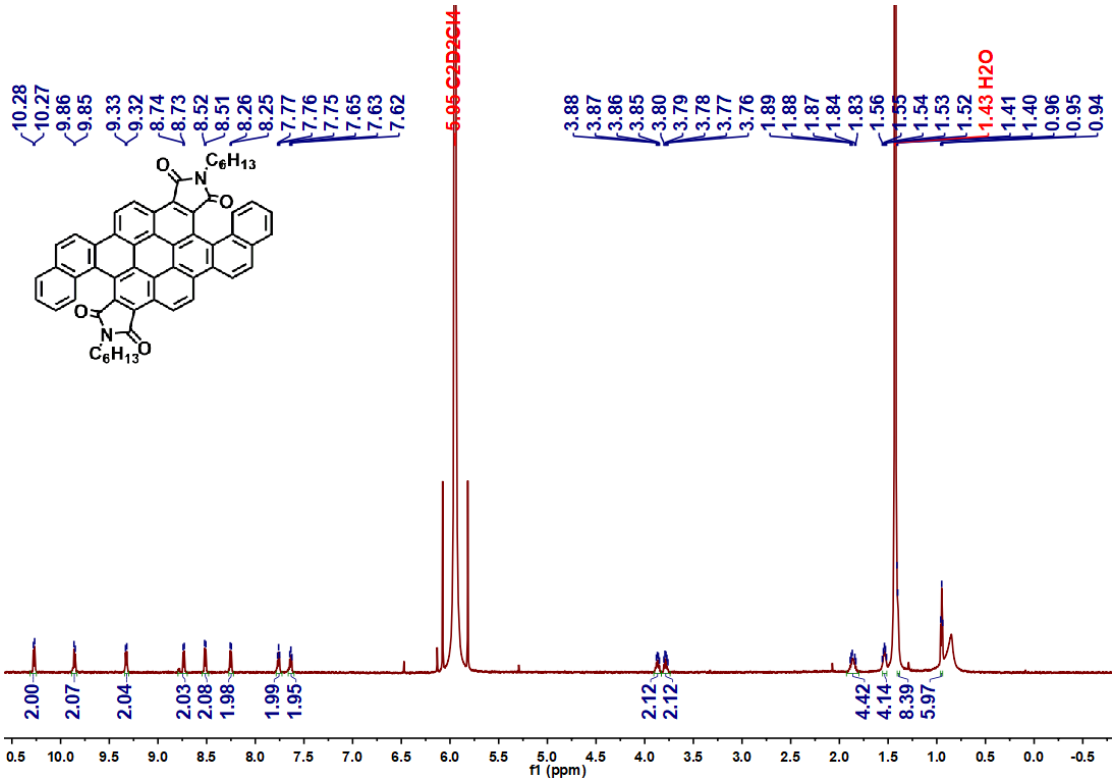

Figure S43. ^{1}H NMR spectrum of compound **3** (700 MHz, $C_2D_2Cl_4$, 373.2 K).

11 Reference

S1. Murai, M.; Iba, S.; Ota, H.; Takai, K. *Org. Lett*. 2017, **19**, 5585.

S2. Frisch, M. J.; Trucks, G. W.; Schlegel, H. B.; Scuseria, G. E.; Robb, M. A.; Cheeseman, J. R.; Scalmani, G.; Barone, V.; Mennucci, B.; Petersson, G. A.; Nakatsuji, H.; Caricato, M.; Li, X.; Hratchian, H. P.; Izmaylov, A. F.; Bloino, J.; Zheng, G.; Sonnenberg, J. L.; Hada, M.; Ehara, M.; Toyota, K.; Fukuda, R.; Hasegawa, J.; Ishida, M.; Nakajima, T.; Honda, Y.; Kitao, O.; Nakai, H.; Vreven, T.; Mont-gomery, J. A., Jr.; Peralta, J. E.; Ogliaro, F.; Bearpark, M.; Heyd, J. J.; Brothers, E.; Kudin, K. N.; Staroverov, V. N.; Kobayashi, R.; Nor-mand, J.; Raghavachari, K.; Rendell, A.; Burant, J. C.; Iyengar, S. S.; Tomasi, J.; Cossi, M.; Rega, N.; Millam, N. J.; Klene, M.; Knox, J. E.; Cross, J. B.; Bakken, V.; Adamo, C.; Jaramillo, J.; Gomperts, R.; Stratmann, R. E.; Yazyev, O.; Austin, A. J.; Cammi, R.; Pomelli, C.; Ochterski, J. W.; Martin, R. L.; Morokuma, K.; Zakrzewski, V. G.; Voth, G. A.; Salvador, P.; Dannenberg, J. J.; Dapprich, S.; Daniels, A. D.; Farkas, Ö.; Foresman, J. B.; Ortiz, J. V.; Cioslowski, J.; Fox, D. J. *Gaussian 09*, Revision E.01; Gaussian, Inc.: Wallingford, CT, 2013.

S3. (a) Lee, C.; Yang, W.; Parr, R. G., *Matter Mater. Phys.* 1988, ***37***, 785. (b) Miehlich, B.; Savin, A.; Stoll, H.; Preuss, H., *Chem. Phys. Lett.* 1989, ***157***, 200. (c) Becke, A. D., *J. Chem. Phys.* 1993, ***98***, 5648. (d) Grimme, S.; Ehrlich, S.; Goerigk, L., *J. Comput. Chem.* 2011, ***32***, 1456. (e) Grimme, S.; Antony, J.; Ehrlich, S.; Krieg, H., *J. Chem. Phys.* 2010, ***132***, 154104.

S4. Weigend, F.; Ahlrichs, R. *Phys., Chem. Chem. Phys.* 2005, ***7***, 3297-3305.

S5. (a) Hehre, W. J.; Ditchfield, R.; Pople, J. A., *J. Chem. Phys*. 1972, ***56***, 2257. (b) Hariharan, P. C.; Pople, J. A., *Theor. Chim. Acta.* 1973, ***28***, 213.

S6. Martin, R. L., *J. Chem. Phys*. 2003, ***118***, 4775.

S7. Gaussian 09, Revision D.01, Frisch, M. J.; Trucks, G. W.; Schlegel, H. B.; Scuseria, G. E.; Robb, M. A.; Cheeseman, J. R.; Scalmani, G.; Barone, V.; Mennucci, B.; Petersson, G. A.; Nakatsuji, H.; Caricato, M.; Li, X.; Hratchian, H. P.; Izmaylov, A. F.; Bloino, J.; Zheng, G.; Sonnenberg, J. L.; Hada, M.; Ehara, M.; Toyota, K.; Fukuda, R.; Hasegawa, J.; Ishida, M.; Nakajima, T.; Honda, Y.; Kitao, O.; Nakai, H.; Vreven, T.; Montgomery, Jr., J. A.; Peralta, J. E.; Ogliaro, F.; Bearpark, M.; Heyd, J. J.; Brothers, E.; Kudin, K. N.; Staroverov, V. N.; Keith, T.; Kobayashi, R.; Normand, J.; Raghavachari, K.; Rendell, A.; Burant, J. C.; Iyengar, S. S.; Tomasi, J.; Cossi, M.; Rega, N.; Millam, J. M.; Klene, M.; Knox, J. E.; Cross, J. B.; Bakken, V.; Adamo, C.; Jaramillo, J.; Gomperts, R.; Stratmann, R. E.; Yazyev, O.; Austin, A. J.; Cammi, R.; Pomelli, C.; Ochterski, J. W.; Martin, R. L.; Morokuma, K.; Zakrzewski, V. G.; Voth, G. A.; Salvador, P.; Dannenberg, J. J.; Dapprich, S.; Daniels, A. D.; Farkas, O.; Foresman, J. B.; Ortiz, J. V.; Cioslowski, J.; Fox, D. J. Gaussian, Inc., Wallingford CT, 2013.

S8. (a) Zhao, Y.; Truhlar, D. G. *Acc. Chem. Res*. 2008, ***41***, 157. (b) Zhao, Y.; Truhlar, D. G. *Theor. Chem. Acc*. 2008, ***120***, 215.

S9. For the 6-31G(d) basis set, see: (a) Ditchfield, R.; Hehre, W. J.; Pople, J. A. *J. Chem. Phys.* 1971, ***54***, 724. (b) Hehre, W. J.; Ditchfield, R.; Pople, J. A. *J. Chem. Phys.* 1972, ***56***, 2257. (c) Hariharan, P. C.; Pople, J. A. *Theor. Chim. Acta* 1973, ***28***, 213. (d) Dill, J. D.; Pople, J. A. *J. Chem. Phys.* 1975, ***62***, 2921. (e) Francl, M. M.; Pietro, W. J.; Hehre, W. J.; Binkley, J. S.; Gordon, M. S.; DeFrees, D. J.; Pople, J. A. *J. Chem. Phys.* 1982, ***77***, 3654. (f) Hehre, W. J.; Radom, L.; Schleyer, P. v. R.; Pople, J. A. Ab Initio Molecular Orbital Theory; Wiley: New York, 1986.

S10. Jönsson, U.; Olofsson, G.; Malmqvist, M.; Rönnberg, I., *Thin Solid Films* 1985, ***124***, 117-123.

S11. Glass, N. R.; Tjeung, R.; Chan, P.; Yeo, L. Y.; Friend, J. R., 2011, ***5*** , 36501-365017.
S12. Paterson, A. F.; Faber, H.; Savva, A.; Nikiforidis, G.; Gedda, M.; Hidalgo, T. C.; Chen, X.; McCulloch, I.; Anthopoulos, T. D.; Inal, S., *Adv Mater*. 2019, ***31***, 1902291.